Talanta 236 (2022) 122823

Contents lists available at ScienceDirect

Talanta

journal homepage: www.elsevier.com/locate/talanta

Applied surface enhanced Raman Spectroscopy in plant hormones detection, annexation of advanced technologies: A review

Syed Muhammad Zaigham Abbas Naqvi [a,b], Yanyan Zhang [a,b], Shakeel Ahmed [a,b], Mukhtar Iderawumi Abdulraheem [a,b,c], Jiandong Hu [a,b,*], Muhammad Naveed Tahir [d], Vijaya Raghavan [e]

[a] Department of Electrical Engineering, Henan Agricultural University, Zhengzhou, 450002, China
[b] Henan International Joint Laboratory of Laser Technology in Agriculture Sciences, Zhengzhou, 450002, China
[c] Oyo State College of Education, Lanlate, 202001, Nigeria
[d] Department of Agronomy, PMAS-Arid Agriculture University Rawalpindi, 46300, Pakistan
[e] Department of Bioresource Engineering, Faculty of Agriculture and Environmental Studies, McGill University, Sainte-Anne-de-Bellevue, QC, H9X 3V9, Canada

ARTICLE INFO

Keywords:
Surface enhanced Raman spectroscopy
Nanoparticles
Plant hormones detection
Microfluidic system
Raman active substrate

ABSTRACT

Plant hormones are the molecules that control the vigorous development of plants and help to cope with the stress conditions efficiently due to vital and mechanized physiochemical regulations. Biologists and analytical chemists, both endorsed the extreme problems to quantify plant hormones due to their low level existence in plants and the technological support is devastatingly required to established reliable and efficient detection methods of plant hormones. Surface Enhanced Raman Spectroscopy (SERS) technology is becoming vigorously favored and can be used to accurately and specifically identify biological and chemical molecules. Subsistence molecular properties with varying excitation wavelength require the pertinent substrate to detect SERS signals from plant hormones. Three typical mechanisms of Raman signal enhancement have been discovered, electromagnetic, chemical and Tip-enhanced Raman spectroscopy (TERS). Though, complex detection samples hinder in consistent and reproducible results of SERS-based technology. However, different algorithmic models applied on preprocessed data enhanced the prediction performances of Raman spectra by many folds and decreased the fluorescence value. By incorporating SERS measurements into the microfluidic platform, further highly repeatable SERS results can be obtained. This review paper tends to study the fundamental working principles, methods, applications of SERS systems and their execution in experiments of rapid determination of plant hormones as well as several ways of integrated SERS substrates. The challenges to develop an SERS-microfluidic framework with reproducible and accurate results for plant hormone detection are discussed comprehensively and highlighted the key areas for future investigation briefly.

1. Introduction

Phytohormones are those trifling elements which are structurally unrelated but critically important to regulate plant growth plasticity [1] in response to environmental stimuli by taking adaptive measures in adverse conditions [2,3]. Five classical plant hormones are known as ethylene, auxin, gibberellins (GA), cytokinins (CKs), and abscisic acid (ABA). Later research extended phytohormones' circle by discovering salicylic acid (SA), strigolactones (SLs), Brassinosteroids (BRs) and jasmonates (JAs) [2,4]. Research analysis, identification and efficient detection and monitoring have revealed critical importance of endogenous plant hormones.

A journey from plant hormones discovery till now has made strong instrumental development with mature and specific plant hormones analysis, i.e. gas chromatography-mass spectrometry (GC-MS), capillary electrophoresis (CE) [5], enzyme-linked immune sorbent assay (ELISA) [6], ultra-performance liquid chromatography-mass spectrometry (UPLC-MS) [7], high performance liquid chromatography-mass spectrometry (HPLC-MS) [8,9], liquid chromatography-ultraviolet detection (LC-UV) [10] and so on. Modern analytical techniques should have a

* Corresponding author. Department of Electrical Engineering, Henan Agricultural University, Zhengzhou, 450002, China.
E-mail addresses: zaigham572@163.com (S.M.Z.A. Naqvi), zyanyan0923@163.com (Y. Zhang), shakeel.ahmed@qq.com (S. Ahmed), m.iderawumi@gmail.com (M.I. Abdulraheem), jdhu@henau.edu.cn (J. Hu), naveed@uaar.edu.pk (M.N. Tahir).

https://doi.org/10.1016/j.talanta.2021.122823
Received 2 June 2021; Received in revised form 20 August 2021; Accepted 22 August 2021
Available online 25 August 2021
0039-9140/

high degree of specificity and sensitivity, identify and quantitative analysis. They should target analytes with the lowest sample pretreatment requirements, and discuss the dual nature of plant hormones as inhibitors and activators of plant growth and development as well [11–15]. Lack of rapid, selective and sensitive detection of chemical species in current methods lead to the development of advanced SERS techniques [16].

Amongst most of the available technologies, Raman technique has proven to be a significant substitute to provide non-destructive, fast and precise analysis. Raman technique also becomes unique from other technologies due to its least required sample preparations and handlings. Raman's inelastic scattering provides ample spectral information about molecules, and the distinctive spectrum acquired can specifically identify the specific element in composite matrices, i.e. food, organisms and materials [17]. However, a vital drawback of conventional Raman is that inelastic scattering process is weak, resulting in weak signals that ultimately limit the Raman applications and make the detections difficult. Contrastingly, this spectrum of weak signals can hardly be disturbed by water that shows great potential of Raman utilization in aqueous systems [18]. Conducive to expand the utilization of Raman technique, numerous strategies have been established to enhance the signal strength. Amongst the most important techniques to amplify Raman scattering is SERS, which has a very high Raman signal intensity and exhibits a significant enhancement factor (EF) reaching 10^{11} [19].

SERS is an amplification of the inelastic scattering of light at molecules on metal surfaces of nanostructures [20]. Its versatile analytical technique in which laser excites vibrational transition in nanostructure plasmonic metal creates Raman signals to form a characteristic spectrum or "molecular fingerprint" [21,22]. Weak Raman signals of molecules are amplified by avoiding strong background fluorescence and excited plasmonic resonance, as a result, SERS can directly determine picomoles to femtomoles of analyte in samples [23,24]. Furthermore, preparation of complex structures for advanced optoelectronic and microfluidic applications has become far easy and versatile because laser can make periodic patterned structures with nanoparticles (NPs) and they can be utilized in SERS determinations [25–27]. However, spatially and spectrally correlated SERS and surface plasmon resonance spectra are needed to be optimized with the excitation laser wavelength [28,29].

Under the stimulation of incident light at a certain wavelength, conductive electrons strongly generate the electric field on the surface of plasmonic nanostructures [30,31]. Plasmonic nanostructures with certain textures and structures elevate the sensitivity of SERS-based molecular analysis, as well as Raman intensity is enhanced [32]. Unique optical properties of gold (Au) and silver (Ag) made them widely used NPs in plasmonic resonance techniques. Light strongly scattered by plasmon NPs leads to localization, quantification and molecular imaging of analytes [33]. Ranging from nanospheres to nanowires, hollow nanocages, high aspect ratio nanorods (NR), and top-down nanochips deposited, plasma NP structures are modified according to the requirement [34]. Molybdenum disulfide (MoS_2) based nanohybrids and novel green method (photochemical reduction of femtosecond laser pulses) are certain examples of enhancing chemical catalytic performances of modified plasmonic NPs with distinguished biochemical sensing properties [35].

Surface modification is another approach to enhance the SERS substrates' stability and uniformity and its activity during the SERS detection process. These modifications are achieved by creating SERS-active "hot spots" in adjacent metal NPs at a sufficiently close distance [36,37]. Various SERS applications are in run with these modifications yet in order to achieve high signal enhancement factors (EF) and uniformity in analytical approach consistent and low-cost substrates are in deep demand [38]. Various SERS-active substrates are now in action with greater sensitivity and signal enhancement by utilizing surface modification or immobilization [39]. Rough metal surfaces of different shapes and sizes under different conditions came in form by electrochemical deposition of gold, silver, lithium, copper or colloids of other metal particles [40] and by polymerization methods as well [41]. The localized surface plasmon resonance (LSPR) of the plasmonic molecule NP caused a remarkable enhancement of SERS of the target molecule, which was subjected to the contribution of the metal to the charge transfer of the target molecule [42]. In non-plasmonic conditions, SERS is thought to be related to the Charge-transfer (CT) transition, which is called chemical enhancement (CE) [43]. It is not always easy to single out the ones, which belonged to Raman enhancement, the reason CE known to occur asymmetrical. CE effect can be briefly described by specific interactivity among molecules and surfaces which includes CT, exchange or covalence [44–47].

The application of different forms of plasmonic nanoparticles to prepare SERS substrates and use of different excitation ranges of laser spectra in the detection of plant hormones will be discussed in this review. This study targets the improved designs of SERS substrates and their reliable synthesis to increase the market value by using plasmonic nanoparticles for plant hormone detection. Finally, the emerging trends and challenges and future directions in the detection of plant hormones using SERS are mentioned in the conclusion section. This review paper further tends to study the fundamental working principles, methods, applications of SERS systems and their execution in experiments of rapid determination of plant hormones using several ways of integrated SERS substrates.

2. SERS: A revolution in laser detection

Since the evolution of SERS on a rough Ag metal surface in 1970, material sciences, life sciences, biochemistry and field of chemistry have modernized in rapid detection applications. Because Raman scattering is a phenomenon of gain of energy (anti-Stokes) or energy loss (Stokes) of inelastic scattering of photons through plasmon nanostructures which enables sensitive and real-time detection up to single molecular level [48–51]. This change of energy is called Raman shift and possesses an expression as follows

$$\Delta\omega\left(cm^{-1}\right) = \left(\frac{1}{\lambda 0(nm)} - \frac{1}{\lambda 1(nm)}\right) \times \frac{\left(10^{7} nm\right)}{(cm)} \tag{1}$$

where.

λ_0 is denoted for incident wavelength

λ_1 is denoted for scattered Raman wavelength [32].

Raman phenomenon is a light interaction process with molecules comprised of two steps (1) excitation process (2) emission process [52,53]. Both molecular specificity and high enhancement factors are gained using engineered plasmonic surfaces in numerous bioanalytical applications that make Raman scattering a powerful analytical tool [54]. As a result of electromagnetic radiation at metal-dielectric interface, adjacent molecules of surface plasmons (SPs) are excited and Raman signals are enhanced significantly [55–57]. Principle illustration of Raman process is expressed in a schematic diagram (Fig. 1) [32].

SERS intensity of a molecule is briefed by the following expression [58],

$$P \propto N \cdot \sigma_{SERS} \cdot \frac{|E_{loc}|^4}{|E_0|^4} \cdot |E_0|^2 \tag{2}$$

where.

N determined numbers of scatterers of laser focal volume.

E_{loc} is for enhanced amplitude of electric field

σ_{SERS} denoted the factor of chemical enhancement.

E0 denoted the incident electrical field.

P is power of enhanced Raman radiation.

2.1. Enhancement mechanism in SERS

SERS can precisely improve SERS signals of molecules adjacent to

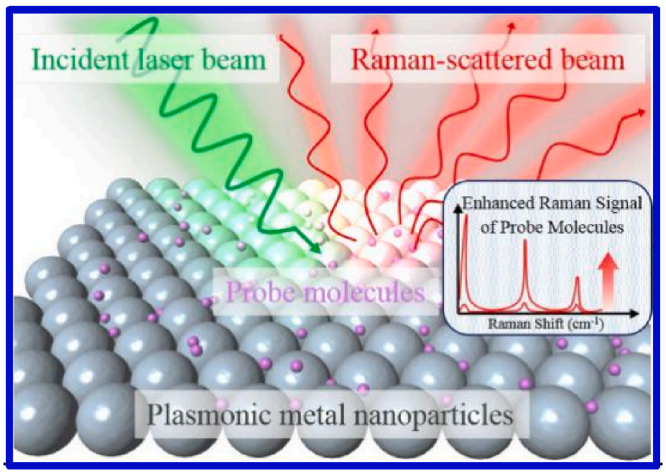

Fig. 1. Principle illustration of surface enhanced Raman scattering process. Combination of plasmonic nanoparticles and laser excitation wavelength on rough metal surfaces generate Raman scattered beam. Rough metal surfaces further help to amplify weak Raman signals [32].

metal nanostructures [59–61]. Moskovits (1978) explained the EM mechanism phenomenon of SERS first time in 1978 [62] and later on briefed by Kerker [63]. Though, three mechanisms of Raman signal enhancement have been discovered (I) electromagnetic enhancement [62,64], (II) chemical enhancement [65] and (III) Tip-enhanced Raman spectroscopy (TERS) [66] yet particular enhancement mechanism is still a debatable study [67–69].

2.1.1. Electromagnetic enhancement

Raman enhancement by plasmon resonance excitation is commonly denoted as electromagnetic enhancement which contributes about 10^4–10^7 of enhancement mechanism in SERS [70–75]. EM enhancement is a result of excited plasmonic metal NPs and detailed temporal and spectral changes of single molecular function in SPs are reported by SERS spectroscopy [54,76]. Near a graphene waveguide, when the donor and acceptor are localized to the waveguide, SPs lead to an increase in the electromagnetic energy transfer rate in a theoretical study [77]. Many scientists have done experimental studies to investigate electromagnetic phenomenon. .On the top of the list Kall and his colleagues' work is recognized, who in 1999 analyzed and solved the complete electrodynamic equation related to the generalized Mie theory. They further calculated the local field enhancement in the silver nanosphere dimer [52]. For isolated molecules (a) and clusters (b), it is observed that the Raman spectra calculated utilizing time-dependent density functional theory (TDDFT) are similar (Fig. 2) [78,79].

A novel method in SERS is getting rise in which plasmonic properties are tuned by polarization of incident light and surface is programmed by gradient permittivity of material (Fig. 3) [80]. Enhanced SERS performance in literature has been reported when SP wavelength (λ_{SP}) of the nanostructure was amongst excitation wavelength (λ_{exc}) and Raman signal wavelength λ_{RS} [75,81–84].

SERS activity in tunable silver nanodomes (AgNDs) was enhanced up to two orders of magnitude (analytical enhancement factor (AEF), 6.05 $\times$ 10^6) because intense E-field was distributed amongst neighboring AgNDs and AgNDs. λ_{LSPR} was present in-between λ_{exc} and λ_{RS} [85] (Fig. 4). Therefore, in EM mechanism significant, Raman enhancement is described as a response of surface plasmon resonance generated due to the plasmon energy of noble metals when meet to the excitation energy of lasers [86].

2.1.2. Chemical enhancement

Chemical enhancement (CE) is a mechanism of SERS enhancement considered advanced and mandatory part of plasmonic EM theory which depends not only substrate but analyte molecules as well [87]. Stronger enhancement of pyridine compared to water [88] was not explainable

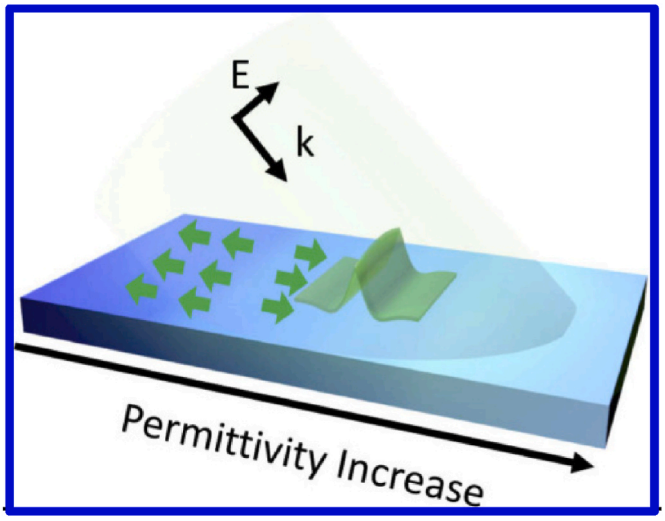

Fig. 3. Schematic illustrating localization of field and effects of enhancement on gradient permittivity material. Free-space light stimulates surface plasmon polaritons (SPPs) that proliferated in two dimensional directions along permittivity gradient. Excited SPPs propagated in the directions of green arrows and enhancement and localization of SPPs is directed toward green wave [80]. (For interpretation of the references to color in this figure legend, the reader is referred to the Web version of this article.)

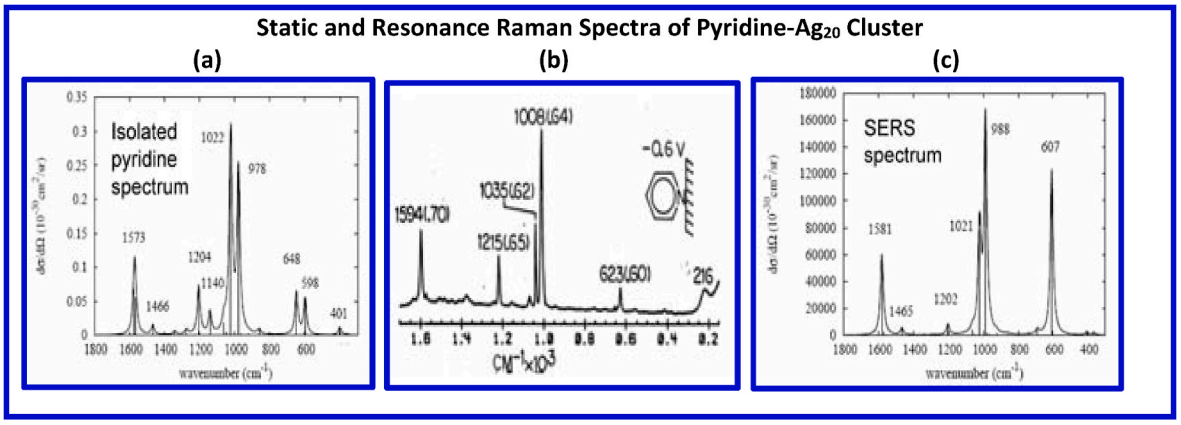

Fig. 2. (a) TDDFT spectra of pyridine. (b) The SERS results of the experiment. (c) pyridine/silver complex [78].

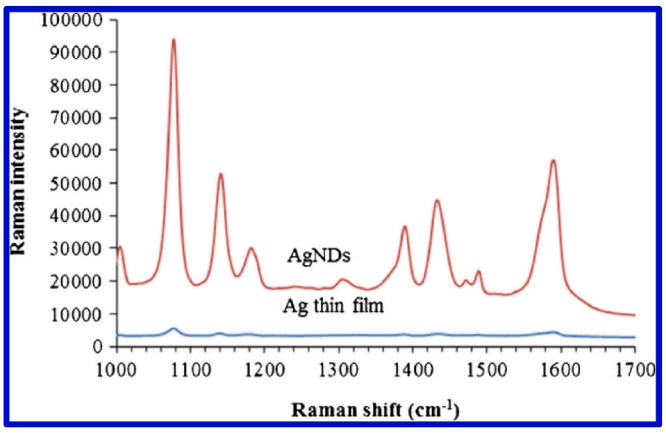

Fig. 4. Illustration of Raman signals of 4-ATP molecules congregated on AgNDs and Ag thin film [85].

only by EM mechanism [78] which lead to an incipient study of chemical mechanism (CM) based enhancement [47,89–91] and named as "first layer effect" [89,90].

Charge-transfer (CT) mechanism is well recognized phenomenon in SERS chemical enhancement. Electrolyte ions are fundamental in CT complexes, either formed by direct (covalent) or indirect binding, to create hot spots by aggregating NPs [92–96]. Analyte molecule when binds to a nanostructured noble metal surface, weak Raman signal can be intensified by factor of 10^8 [97]. CE includes several different transitions/processes that manifests relatively complex enhancing factors [43]. CE tends to be varied depending on metal surface and the CT among the substrate and the adsorbed molecule (Fig. 5) [98,99].

CT efficiency and modified chemical active sites in semiconductors substrates are important factors of SERS enhancements [101–104]. Charge transition behaves differently for dielectric substrates. In this case, valence band (VB) of substrates and lowest unoccupied molecular orbital (LUMO) of molecules as well as highest occupied molecular orbital of molecules and conduction band (CB) edge of substrates become critically important factors. CT in metals occurs between fermi level and highest occupied molecular orbital of analytes [105–107]. Chemical enhancement can be significantly improved by solvent environment for both non-resonance enhancing in Raman signals of chemical bonds and resonance SERS enhancing of photo-excited CT [108–110].

Chemical interface damping was recognized as new technique under resonant condition in which CE contribution to the SERS signal can be quantified and tuned selectively [111–113]. Largest enhancement factor reached to 2.5 in a study of SERS measurement for Rhodamine 6G (R6G) molecules with tuned N-doped graphene (NGs) substrate. By using the electric field effect to adjust the graphene Fermi level, enhanced magnitude was found to be greater than Raman modulation (Fig. 6). Tunable graphene enhanced Raman scattering eventually expressed itself being chemical enhancement mechanism derived from the CT settled among substrate and probe molecule [114–116].

2.1.3. *Tip-enhanced Raman Spectroscopy*

Tip-enhanced Raman spectroscopy (TERS) is specialized method of SERS in which Raman enhancement only occurs on the sharp pin (coated with gold) to the closest atoms [117]. This technique was first proposed by Wessel in 1985 by achieving single point enhancement using scanning probe microscopy (SPM) near the apex of the plasmonic nanotip (Fig. 7) [66,118,119]. By positioning and raster scanning nanotip on a sample, high spatial resolution of 20–30 nm can be achieved. While

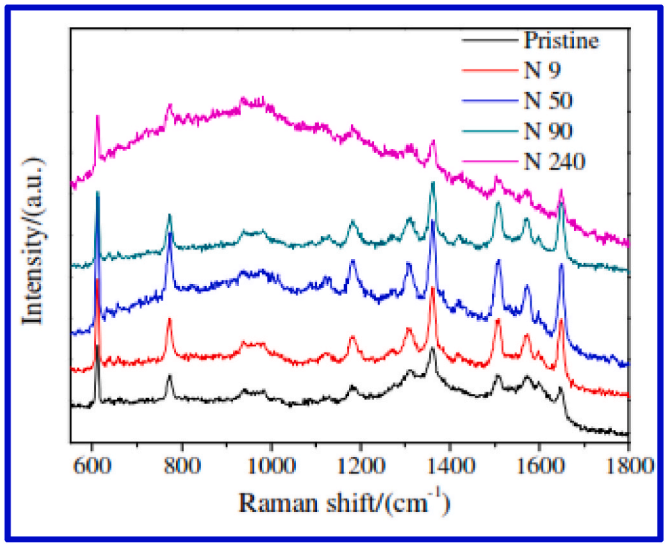

Fig. 6. Raman bands of R6G molecules with an adsorption concentration of 5 × 10^{-7} M on the pristine and nitrogen-doped graphene. The relative EF of the five bands increase with the increase of N-content, and the maximum EF related to NG can reach 2.5 and after that decrease. In all cases integration time was 8 s [116].

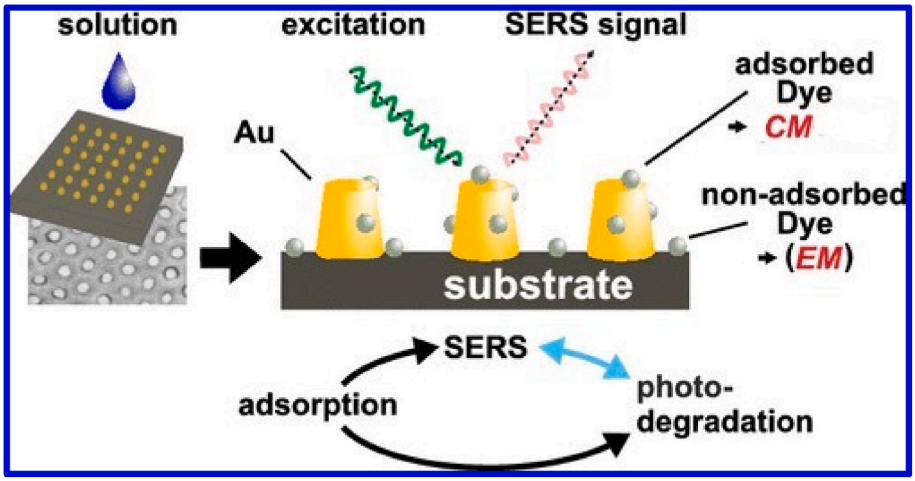

Fig. 5. Analysis of photo-degradation model producing CE in SERS. The energy of the excitation laser is far less than the energy of the substrate surface plasmons. SERS is believed to be related to the charge transfer transition [100].

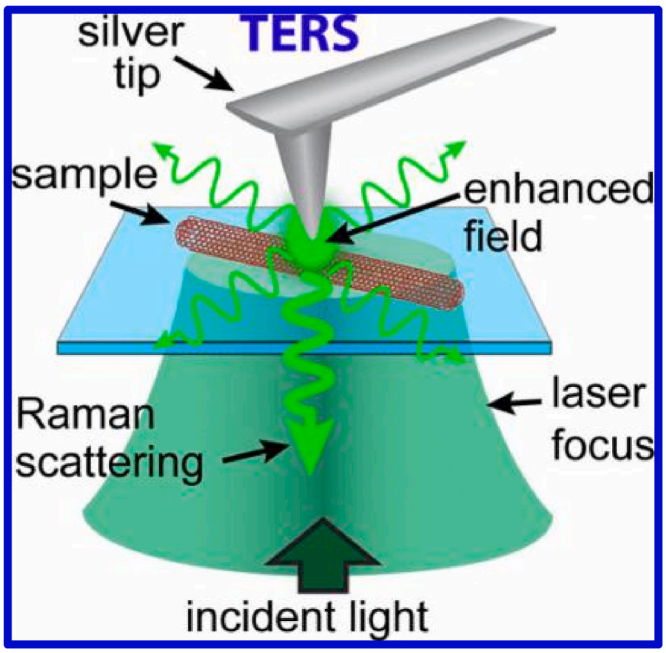

Fig. 7. Schematic diagram of Tip-enhanced Raman spectroscopy [119]. According to sample size and incident wavelength, 0.5–1.0 μm spot sized diffraction limit is generated by bringing SERS active tip within laser spot on samples.

enhancement factor of about 10^3 – 10^6 can measure weak phonon modes from jot of samples [120–124].

TERS technique combines atomic force microscopy (AFM) [125] or scanning tunneling microscopy (STM) [126] with Raman spectroscopy. Fundamentally two factors, plasmonic probe tip material and tip-sample distance, generates the stable and reproducible Raman enhancing spectra [127,128]. Generally Au tips are utilized for excitation range of 633–785 nm. Enhancement factor in graphs (Fig. 8) for 488 nm excitation wavelength with silver tips was performed in which excitation wavelength can vary up to 568 nm. Stable and reproducible signal intensity is dependent on surface plasmons at the tip apex [118,129–131]. Plasmonic tip perceives Raman scattering by a far-field detector and TERS enhancement is maximized by collecting/dispersing proficiency of plasmonic tip from/to the far field which is the fundamental principle of TERS [129,132].

2.2. Setup configuration of SERS (laser, excited beam and emission wavelengths)

Raman Effect is the fundamental principle of Raman spectroscopy in which inelastic scattering of photons from a Raman active sample occurs [133,134]. Excitation photons from a laser of calibrated frequency and polarization in range of UV–Vis-IR scatter from molecules [135–137]. Resulted "Raman shift" in Raman Spectroscopy integrated with metal surface (nano) technology explicated a powerful analytical tool named "Surface Enhanced Raman Spectroscopy" [138–140]. Raman signals raised are intrinsically very week in nature. In case of fluorescent compounds weak Raman signal is concealed by fluorescence signals [141–143]. Strong fluorescence signals can be kept at arm's length by selecting appropriate laser excitation wavelength, especially near infrared (NIR) photon selection [144].

Effective Raman hotspots give rise to an ultrahigh Raman scattering generating absorption spectra ranging from 600 to 800 nm for plant hormone detection [145]. Similar SERS spectrum band was observed when 633-nm exciting laser was used at 6 mW power [146]. Efficiency of SERS activity varies with the Raman active molecules in a dispersive Laser Raman system. .In a Laser Raman system (Argon-ion, He–Ne, and diode lasers operating at 514.5 nm, 633 nm and 782 nm excitation wavelength, respectively), Argon-Ion laser has found to be more efficient for non-fluorescent compounds as compared to diode laser. It is given the preference to eliminate characteristic fluorescence of many of the elements in Raman excitation studies [144,147–150]. AgNPs used for localized surface plasmon resonance have a size of 10–30 nm has absorption spectra not more than 450 nm. Absorption wavelength becomes stronger by AgNPs deposition and increased quantity [151,152].

SERS spectra emissions have been recorded for varied excitation wavelength because several SERS active molecules feature different characteristics [153]. Molecular absorption properties close to 1064 nm can enhance resonance, e.g. dye IR-1048 (sigma-Aldrich) has a strong molecular absorption at 1048 nm as compared to dye IR-27 having a maximum absorption at 988 nm [154]. Excitation wavelength at 785 nm may produce SERS signals from these molecules but strong associated fluorescence can mask SERS signals effectively prior to detection. SERS detection may then occur with 1064 nm excitation [155–158].

3. Detection of plant hormones using SERS

Literatures have described two ways of study on plant hormones detection. One is theoretical study and other is practical study. Both are described below to make a compact review for further modifications in SERS enhancements.

3.1. Theoretical studies on the detection of plant hormone using SERS

Plants under biotic and abiotic stresses are severely affected by yield as well as growth and development [159–161]. The stress conditions are efficiently thrived by plants due to a vital and mechanized physiochemical regulations of effector molecules known as plant hormones [162,163]. These secondary metabolites are present in very low concentrations (generally 1 μmol L^{-1}) in plant tissues but produce high bioactive signals [164]. Biosensing analysis applications required to be more specific in detection and imaging of target molecules having narrow Raman vibrational spectra. SERS is a nondestructive biosensing technique to provide specific fingerprint spectrum as well as structure of the target molecule [165–167]. Herein, theoretical studies regarding plant hormone detection using SERS are summarized.

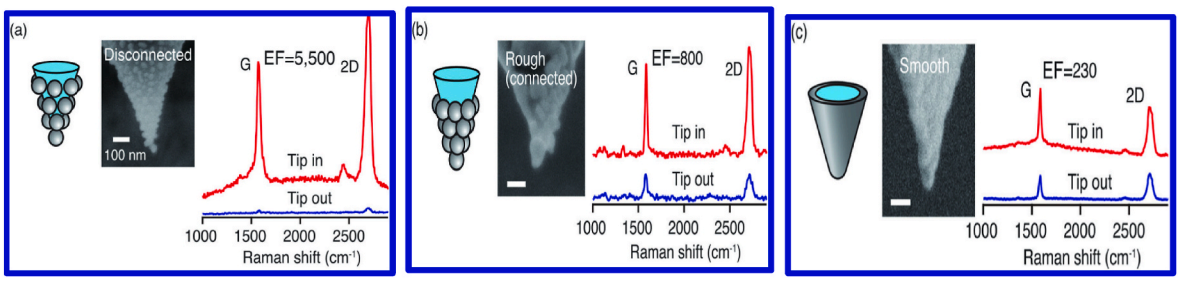

Fig. 8. The enhancement effect of various shapes of Ag probes. (A) Grains arranged discretely on the tip. (B) Rough grooved granular tip. (C) The tip is smooth [118].

3.1.1. Dempster-Shafer theory

Arthur P. Dempster evolved a mathematical evidence theory [168,169] which can infuse combined notions of imprecise, uncertain and incomplete information of different sources [170,171]. Glenn Shafer in 1976 further extended this work [172] and now known as Dempster-Shafer (DS) theory, an extended form of Bayesian probability theory. Fuzzy theory model combined with DS evidence theory for estimation of Auxin-response element (AuxRE) decreased false positive results. A comparison of true and false positive resulted values is attributed in Fig. 9. DS data fusion decreased the false positive percentage to 90% when compared to Method 1 and Method 2 separately presented in the graph. Importance of data fusion with improved reliability of prediction was indicated when credibility value equals 0.9 [173].

3.1.2. Density functional theory

Density functional theory (DFT) computes strategies from obtained information of properties, energies and structures of molecules and atoms [174,175]. Biochemical industry was able to get sharp and clear concepts in chemistry as DFT of molecules and atoms was endorsed by Parr and Yang [176]. DFT theoretically simulated the molecular characteristics and frequency of plant growth regulators (PGRs)-isolated molecules resorted Becke three-parameter Lee-Yang-Parr (B3LYP)/6-31G (d, p) model. According to Fresnel formula, the significant frequencies range of 0.06–4 THz among absorption coefficient and PGRs refractive index were recorded [177,178].

3.2. Experimental studied on the detection of plant hormone using SERS

Plant hormones in low concentration and trace amounts can now be determined by the use of noble metals in SERS which can produce unique spectral fingerprint in a composite matrix [179,180]. Fast, specific and precise SERS investigation of trace N^6 –Benzyladenine, one of the cytokinins with extreme importance in multiple stresses of drought, salinity, temperature extremes and responsible for antioxidant activities in leaves of plants [181], developed an Au colloidal NPs substrate in a complex matrix [182]. Another study proposed certain flavonoids (hesperetin, naringenin, quercetin, and luteolin) detection using silica NPs template to embed silver nanoparticles (SiO_2@Ag@Et-β-CD NPs) that generated hot spots and SERS signals. SERS activity for luteolin determination in terms of selectivity and sensitivity was observed with highest bands. SERS intensity peaks 513, 684, 742, and 1123 cm^{-1} were observed to be increased with the luteolin concentration rage. Normalized SERS intensity in this system for luteolin was observed at 742 cm^{-1} (Fig. 10) and 10^{-7} M limit of detection (LOD) compared to other organic molecules had been observed [183,184].

Novel strategic analogies have been integrated with SERS techniques to assess the plant hormones, though they are not many and can count on the fingers of one hand. A cationic Ehrlich reaction strategy developed to detect indole-3-butyric acid (IBA) plant hormone selectively raised new absorption spectrum of 600–800 nm. Au NPs hotspots, p-(dimethylamino) benzaldehyde Ehrlich reaction and exited laser generated ultrahigh Raman scattering down to nanomolar level having LOD of 2.0 nM IBA. About 97.5%–101% IBA was recovered (Fig. 11). Plant hormonal detection, molecular mechanisms and dynamic assessments to understand wider role and physiochemical importance of plant hormones can easily be assessed by this potential strategy [146].

Using paper strip with immobilized Au-NPs on it, a label free rapid determination method of Brassinosteroids (steroidal phytohormone) was developed. This on-site detection technique of plant tissues

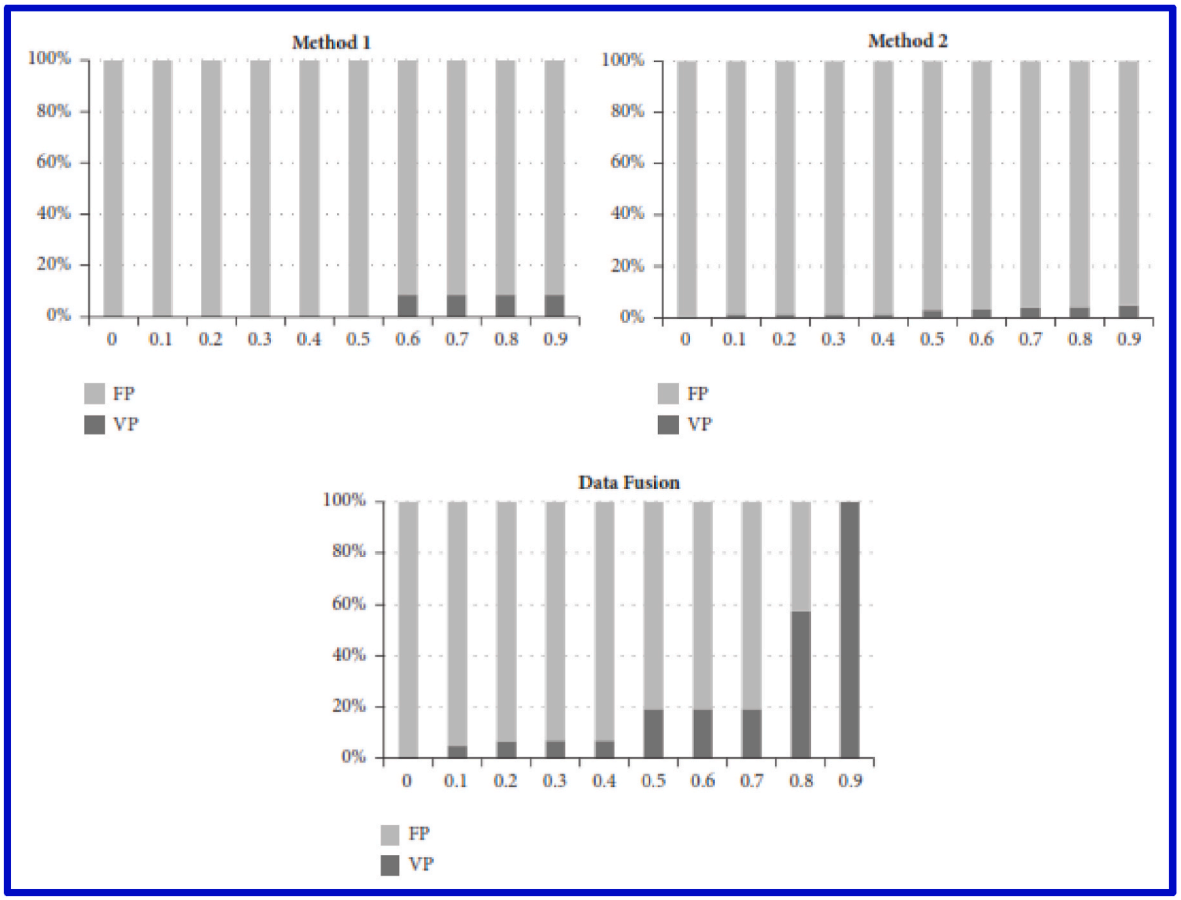

Fig. 9. Before and after data fusion, the progression of positive and false detection values based on credibility value. After data fusion through DS theory combination, the credibility value is equal to 0.9, the number of false positives significantly reduced to the offset point [173].

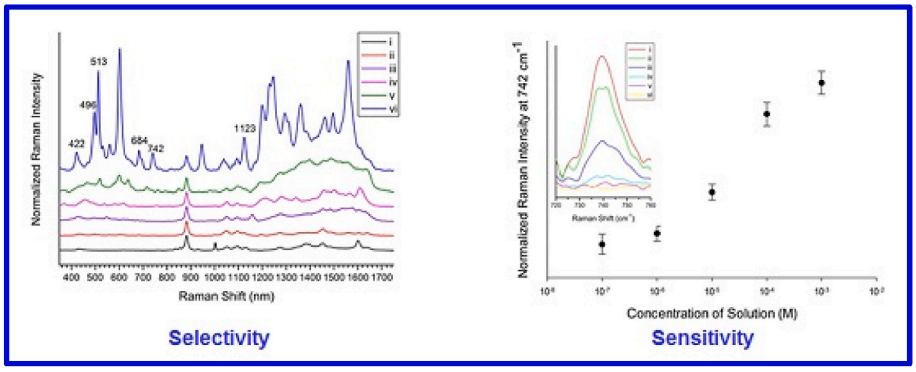

Fig. 10. SERS based flavonoid detection and SERS Selectivity and Sensitivity bands (Selectivity) SERS spectra of (i) Ag NP-bound on silica nanoparticles (SiO_2@Ag NPs), (ii) SiO_2@Ag@Et-β-CD NPs, (iii) SiO_2@Ag@Et-β-CD NPs with Nar, (iv) SiO_2@Ag@Et-β-CD NPs with Hes, (v) SiO_2@Ag@Et-β-CD NPs with Que, and (vi) SiO_2@Ag@Et-β-CD NPs with Lut; (b) SERS spectra (Sensitivity) Normalized SERS intensities at 742 cm^{-1} ((i) 10^{-3} M, (ii) 10^{-4} M, (iii) 10^{-5} M, (iv) 10^{-6} M, (v) 10^{-7} M, and (vi) 0 M) [184].

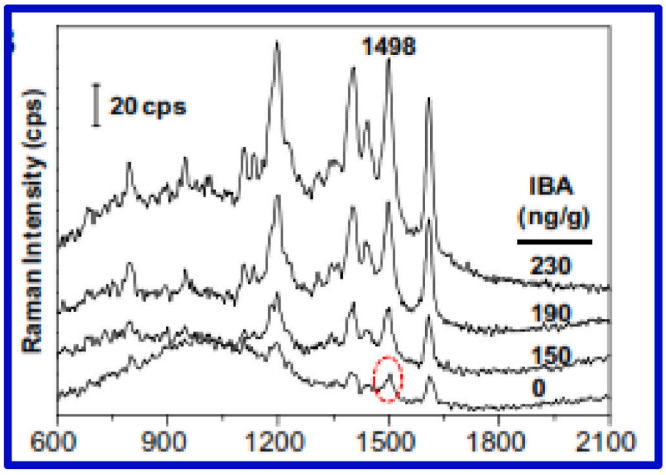

Fig. 11. Au nanoparticles Raman enhancement of mung bean sprout concentrated with IBA in between 600 and 800 nm. Red circle clearly indicated the Raman signal of blank sample at 1498 cm^{-1} [146]. (For interpretation of the references to color in this figure legend, the reader is referred to the Web version of this article.)

possesses many properties e.g. high reproducibility (RSD: 3–13.8%), high EF (1.13×10^8), limit of detection (1×10^{-11}) and more significant value of R^2 (0.99). Moreover, this technique holds a long term stability response to Raman spectrum [185]. Another study used the fibers of filter papers to fabricate AgNPs coated paper for simple and rapid detection. This study not only achieved the lower LODs (10^{-11} and 10^{-10} M) for low abundance molecules but uniform and reproducible detection results were achieved [186].

3.2.1. *Substrates of SERS to plant hormones*

Subsistence molecular properties with varying excitation wavelength require pertinent substrate to detect SERS signals for plant hormone detection. An effective detection of flavonoids was performed on basis of AgNP bound on silica nanoparticles (SiO_2@Ag@Et-β-CD NPs) substrate (Fig. 12). Ethylenediamine-modified β-cyclodextrin (Et-β-CD) served as ligand for flavonoids and to create hotspots and SERS signals Silica NPs served as template for silver NPs embedding. Resulted SiO_2@Ag@Et-β-CD NPs substrate captured Raman signals which indicated the substrate as fast, delicate and discerning sensor to detect flavonoids hormones [183].

The sensitive detection of 6-benzylaminopurine (6-BAP) using SERS, generated significantly improved SERS signals due to use of enhanced substrate of gold colloidal nanoparticle formulated by reducing chloroauric acid with sodium citrate (Fig. 13). The concentration linear of 6-BAP extraction ranged from 0.1 to 5.0 μg mL^{-1}, and peak intensities of SERS signals were observed at 1002, 1318 and 1336 cm^{-1} [188].

Rather than using enhanced substrates, commonly and commercially available substrates can also output significantly enhanced Raman signals, Klarite is among one of them. The Klarite substrate is composed of a silicon surface, forming square assemblage of micron-sized square pyramid voids covered by 300 nm gold coating. They are the commonly used SERS substrate causing the enhancement alongside Klarite pit due to surface plasmons [189–191]. Standard Klarite substrate with a thickness of 300 nm (Fig. 14), contributes minimal for the plasmon effect. The plasmon contribution to electromagnetic enhancement substantially enhances if the gold coating thickens to 125 nm, causing enhancement to almost the double [192].

Paper based substrates has successfully been used with significant LOD in several plant detection techniques. In a paper based substrate, ISSMG method was used in an aqueous media and Au seeds were transferred on paper in the presence of $HAuCl_4$ and $NaBH_4$. In the ISSMG technique paper in vertical position is kept in γ-PGA media, then Au ions are treated with $HAuCl_4$ for deposition of Au particles on paper. $NaBH_4$

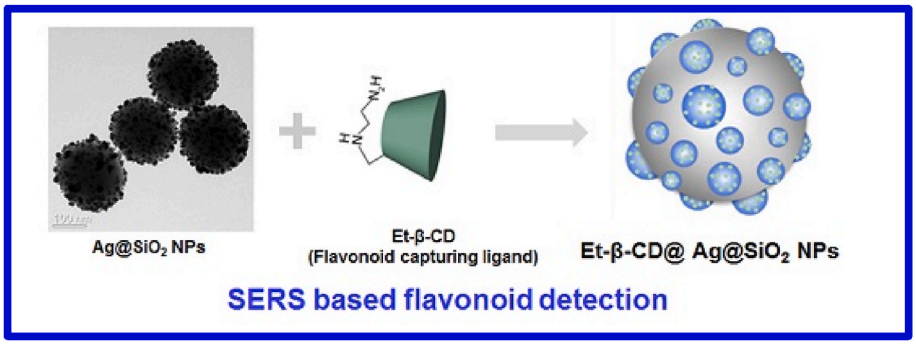

Fig. 12. Et-β-CD immobilized on aggregated Ag-NP bound on silica nanoparticles (SiO_2@Ag@Et-β-CD NPs) act as substrate in SERS analysis of flavonoids determination [183].

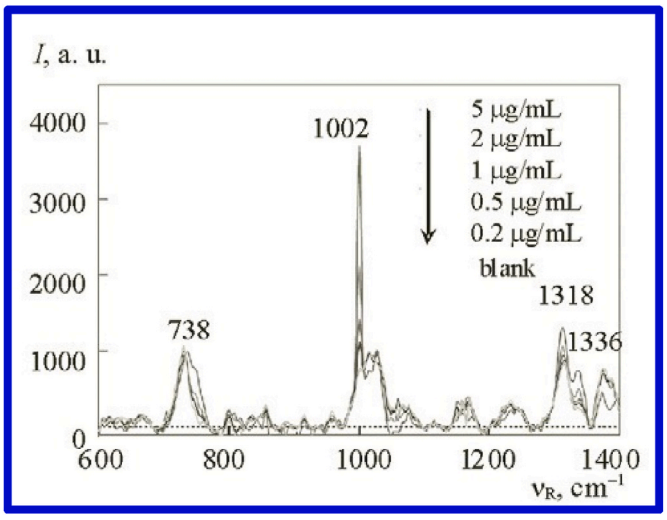

Fig. 13. SERS of 6-BAP: changes in typical Raman shift were recorded at different concentrations of 6-BAP extraction [188].

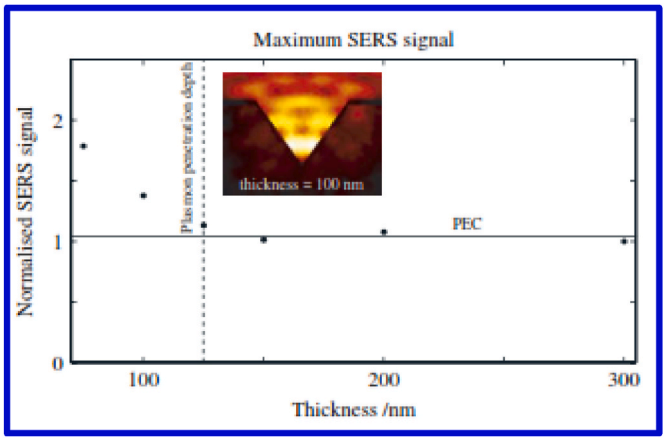

Fig. 14. The relationship between the maximum SERS signal (only electromagnetic enhancement) and the film thickness on the pit wall is normalized to the maximum SERS signal with a metal thickness of 300 nm along the pit wall. Field distribution of a pit with a gold coating of 100 nm thickness showed in an inset of graph [192]. (For interpretation of the references to color in this figure legend, the reader is referred to the Web version of this article.)

is then applied to reduce Au nanoparticles and subsequent washing is done with water to remove strayed particles from solution. Hydrophilic sections are transformed in white color and are activated via gold nanoparticles fabrications that ultimately expressed high EF (1.13×10^8) [185]. Another filter based substrate was produced in which AgNPs were coated on filter papers. AgNPs were deposited in the inner layer of paper and for that purpose, spaces of cellulose structured paper were enlarged by putting it into 0.5 molL^{-1} $AgNO_3$/EG media and then AgNPs were coated [186].

3.2.2. Surface modification of the nano-particles

Nanoparticles with certain surface modifications can amplify SERS signals by generating enhanced plasmon effect from local EM field to rapidly detect the Raman active molecules. Nanogaps can generate a strong EM field where molecules are present to originate strong SERS signals [193]. Moreover, SERS substrates with high molecular concentrations are also responsible for strong signals [194]. Magnetic nanoparticles substrates of transition iron oxide act as contrast enhancement agents. This action occurs due to the surface modifications of magnetic core with pertinent organic or inorganic polymers (i.e. Polyethyleneglycol (PEG), Polyethyleneimine (PEI), Polyvinylalcohol (PVA)) or silica and Au by considering precise and specific chemical and physical properties of metals [195].

Hydrophobic surface modification of substrate is preferably more significant due to efficient amplification of SERS signals. Wettability properties of nanostructures from hydrophilic to hydrophobic are converted by concentrating the diluted analyte in the droplet which can increase surface roughness and bring particle uniformity [196,197]. Heat reflux method was brought under use to modify Ag/ZnO nanocomposites as hydrophobic substrate using a combination of stearic acid (SA) and polyvinylpyrrolidone (PVP) (Fig. 15). Unique surface properties of modified Ag/ZnO nanostructure showed 3-fold signal enhancement and proved as an effective Raman substrate caused by an effect of hydrophobic condensation as compared to hydrophilic Ag/ZnO substrate [198].

Another form of surface modification involves use of citrulline aptamers on the surface of colloidal Ag nanocubes developing a point-of-care (PoC) device. PoC biosensing has ability to detect biomarkers at low concentrations using SERS. This surface modified SERS active substrate had detection ability lowest to 24.5 pM level [199]. Another simple approach for plasmonic NPs surface modification was proposed as a ligand exchange approach using water soluble cationic ammonium pillar [5]arene (AP [5]A). For surfactant-stabilized NPs ligand exchange approach was found to be a difficult surface modification. But SERS efficiency was observed highest for AP [5]A stabilized Au nanospheres (NS) at different excitation wavelengths (Fig. 16). The potential application of detecting different hydrophobic analytes (such as pyrene and pyocyanin) in SERS analysis studies using Au@AP [5]A has achieved LODs of 1 nM and 0.1 mM, respectively [200].

3.2.3. Ligand-based SERS measurement

Solubility, reactivity and surface charge density are the physical and chemical characteristics behind the kinetics of ligand exchange in the surface chemistry of NPs [201–203]. Ligand exchange kinetics has been studied on either bulk metal substrates [204,205] or small metallic nanoparticles (e.g., $Au_{11–140}$, 1–5 nm) [206–208]. Composite patterned SERS signals reflects the ligands collective behavior of ligands packing [209]. Selective detection of specific (α3β1 integrin) exosomes and SERS chemical analysis was illustrated using thiolated peptide ligand attached on silver NPs facet. Jurkat cells which excreted α3β1 integrin negative exosomes didn't show SERS signals as compared to several Raman peaks particular for SKOV-3 exosomes which confirmed importance and sensitivity for this ligand based Raman sensing technique [210]. Capping ligands and nanostars interactions can determine morphology of branched Au nanostars, the colloidal Raman identification of probe molecules at a nanomolar concentration levels. 4-MBA ligands were proven significantly efficient than hydroquinone (HQ) ligand in serrated edged branches of Au nanostars. Moreover, the sharp branched Au nanostars are credible to provide extra SERS activities than roughed surface in numerous ultra-sensitive chemical Raman investigations [211].

A highly specific on-site analysis sensor for copper (Cu^{+2}) detection had applied with detection ability far less than the recommended value of 7.87×10^{-6} M (0.5 μg/mL). Dipicolylamine-based ligand was bound with plasmonic AuNPs to interact with Cu^{+2} which in result confirmed specificity of proposed molecular sensor by making changes in spectral features (Fig. 17). Due to flawless and extraordinary specific and sensitive performance for Cu^{+2}, the demonstrated SERS-based molecular sensors are also feasible for other fields. Moreover, on-site implementations appeared to be viable attributed to flexile and short amount of time to analysis [212].

Sometimes nanoparticles stability limits their application. Therefore, to analyze the myoglobin from a saline solution, bi-ligand technique to silver NPs surface modification was introduced containing two modifiers with thiol groups (3-mercaptopropionic acid (MPA) and thiolated PEG).

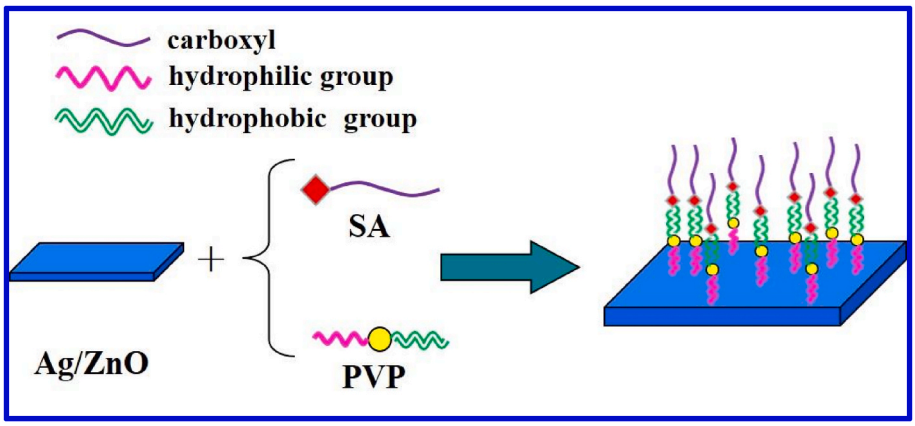

Fig. 15. Schematic diagram of ZnO/Ag substrate by modifying homogenized SA/PVP in a hydrophobic condensation mechanism [198].

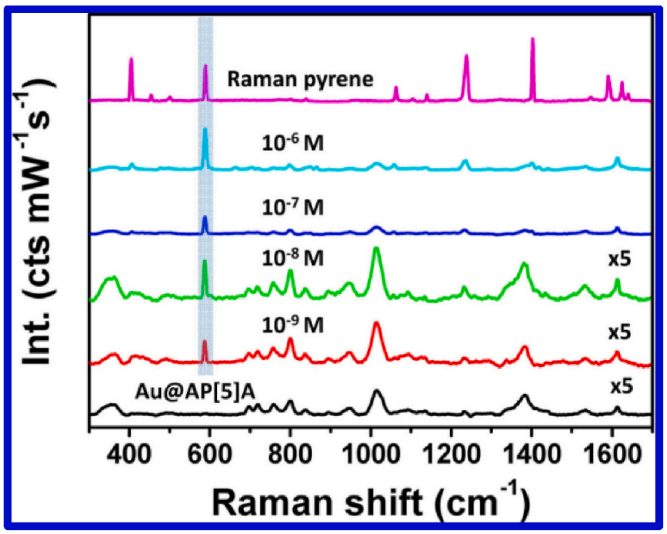

Fig. 16. As shown in the figure, in the presence of 56 nm Au@AP [5]A nanoparticles, the Raman spectra of solid pyrene is on top and concentration range from 10^{-6} M to 10^{-9} M has varied Raman spectra. Excitation wavelength of laser was of 785 nm [200].

Short-chained ligands may be used to regulate selectivity in analysis. Laser-induced sintering was applied to create favorable hotspots. MPA and PEG produced sustainable system when combined by providing adequate time lap for analyte-NP interaction. Resulted Raman spectra thoroughly explained the SERS activity in both deionized (DI) water and saline solution environments (Fig. 18). The functionality of the system demonstrated as an effective technique on Raman analysis and sustaining the colloidal stability in a saline solution [213]. Thus, development of target specific ligands library can rapidly and selectively detect and analyze the target molecules biochemically in a ligand-based SERS measurement [210].

4. Advances in SERS measurements

SERS since its development has many processes of evolutions and now is considered an essential tool in ultrasensitive investigation of small biological molecules, polypeptides and cells as well. The integral SERS fingerprint of polypeptides and lipid bilayers and small molecules enables SERS as label-free techniques of structural information. Moreover, direct sensing, quantification and deeper characterization helps to illustrate the biomolecules near metallic surfaces. Despite such stunning performance SERS measurements were captured in a non-perturbative manner and actual activity spectrum remains submissive. Advances in SERS substrate developments and modifications has changed the face of SERS performance by direct biomolecular quantitation and biophysical characterization more specifically [214].

Although SERS been recognized as ultrasensitive detection tool,

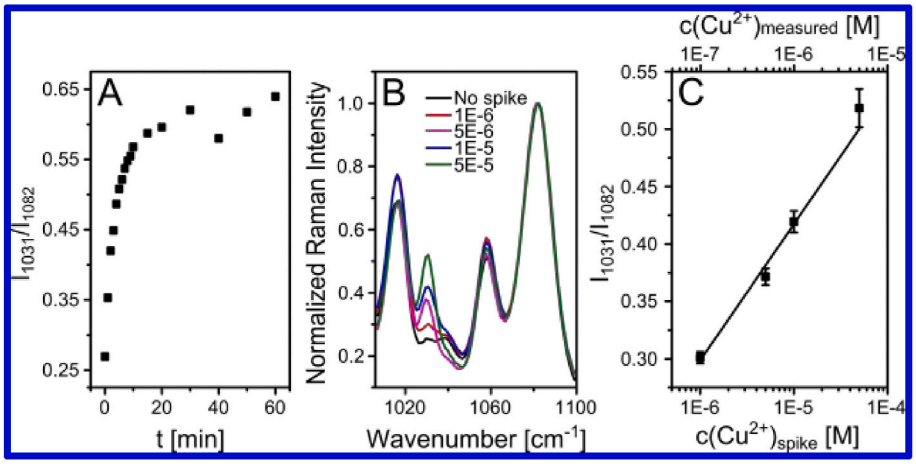

Fig. 17. (A) Time evolution to white wine with 1×10^{-4} M Cu^{+2} for Raman molecular sensor; (B) Response spectrum of Raman molecular sensor to white wine with different concentrations of Cu^{+2} (in M); (C) The response of Raman molecular sensor to Cu^{+2} ions spiked in white wine [212].

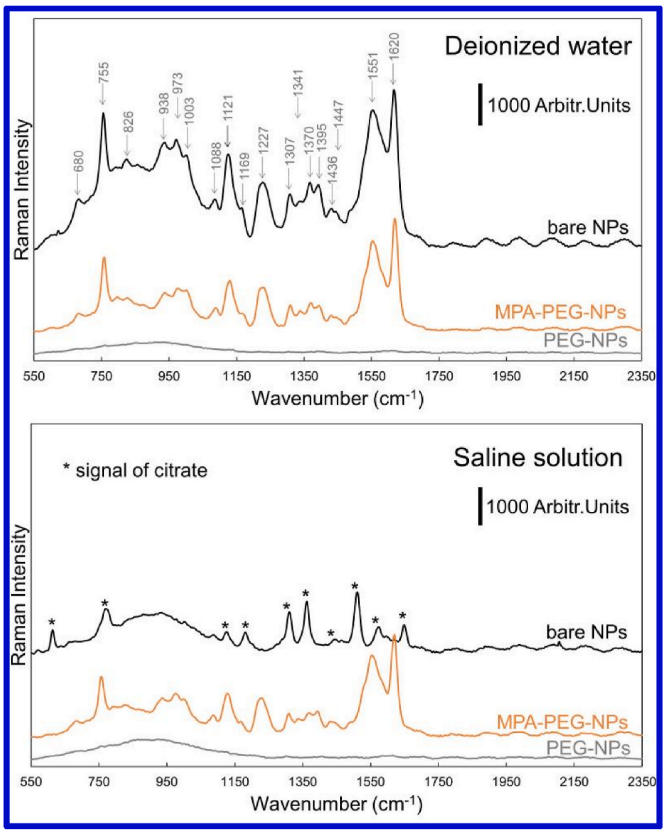

Fig. 18. In deionized water and salt solution, the typical Raman spectra of various surface-modified NPs and myoglobin (50 μM) was observed. Time of exposure was 3 × 10 s with nanoparticle concentration, 3 mg/mL. In order to compare the spectrum better, an offset, background correction and smoothing were applied [213].

problems still exist, i.e. to obtain suitable facsimile among Raman substrate and light and obtaining a stable and sensitive SERS substrate to better enhance the Raman signals, hinder its widespread application or modeling computational electrodynamics. Certain unique advancements in SERS measurements been made to understand the underlying physics, optimal prototype and assembly of Raman substrates for molecular determination. Numerical tools used to model computational electrodynamics are also called algorithm models, are significant methods for calculating parameters related to Raman intensity. It can also be utilized to investigate the electromagnetic field distribution to show optical characteristic spectrum and EF of various substrate fabrications as well. It which can further improve the reproducibility, accuracy and operation stability and solve the SERS problems in electromagnetics [215].

4.1. Algorithms in the SERS measurement

SERS measurements are developed into rapid, specific, sensitive and simple methods when coupled with multivariate calibrations. Raman active substrates with core-shell NPs can produce high enhancement effects for rapid acquisition of Raman spectra. Quantitative analysis and prediction models are further acquired by combining ant colony optimization (ACO), genetic algorithm (GA), Savitzky Golay-First derivative (SG-FD) processing data, linear (partial least square (PLS) and stepwise multiple linear regression (SW-MLR)) and nonlinear (back propagation artificial neural network (BPANN) and backpropagation-adaptive boosting (BP-AdaBoost)) techniques with satisfactory results in verification analysis. A comparative map for different algorithmic measures is here showed with the success results in the recent literature (Fig. 19).

Optical sensors named micro-Raman spectroscopy system are coupled with linear and nonlinear algorithmic models to sensitively and rapidly detect the mercury (Hg^{+2}) residues in dairy products. In a series of events, Au embedded on SiO_2 NPs substrate with EF were generated. ACO and GA were applied to select characteristic variable of SERS spectrum pretreated with SG-FD method to eliminate noise interference. In a subsequent event of modeling PLS and SW-MLR were compared with BPANN and BP-AdaBoost algorithms for pertinent model selection of mercury quantitative determination. Proposed strategy significantly verified the analytical results (significance value. n = 0.05) with inductively coupled plasma mass spectroscopy (ICP-MS) (Fig. 20).

Experimental performance was found significantly improved with ACO algorithm in an ACO-BP-AdaBoost model compared to other quantification models. Higher R^2 value of 0.997 and lower RMSEP value of 0.092 proposed the feasibility of the algorithmic models in detection of heavy metal residues [216].

Combining the chemometric algorithmic models with Raman techniques significantly enhanced the quantification and classification sensitivity of organic and inorganic elements in complex matrix [217]. Chlorpyrifos (CPS) residues detection was performed by developing chemometric algorithms of classification and quantification models with high EF and preprocessed standard normal variate (SNV) Raman spectrum. K-nearest neighbors (KNN) classification model achieved significantly higher classification rates with 90.84–100.00% performance. GA-PLS and synergy interval PLS-GA (siPLS-GA) quantification models exhibited higher R^2 and lower RMSEP values with SNV preprocessed data (Fig. 21) which is a better prediction performance in pesticides residual detection of SERS with effective chemometric models [218].

An efficient diagnostic algorithm was established based on the combination of Raman spectroscopy and Least Absolute Shrinkage and Selection Operator -Partial Least Square Discriminant Analysis (Lasso-PLS-DA) to distinguish blood plasma of cancer patients. Lasso basically performs multiple linear regression based on familiar expressions and its form is:

$$Y = \beta_0 + \beta_1 X_1 + \beta_2 X_2 + \ldots + \beta_n X_n \quad (3)$$

where.

β_0 denotes the residual regression coefficient

β_i is the regression coefficient for 1to n predictor values from data.

X denotes correlation variables of multidimensional data.

Y determines the parameters combination in a regression.

Number of predictive errors in a regression model compare to least square are reduced by Lasso regression. Original *X* correlation variables are optimized in Lasso models by driving the insignificant β values to 0 by weighing more importance to prediction channels and reducing the expected prediction errors. Lasso is represented by following formula:

$$\widehat{\beta}^{lasso} = \arg min_{\beta} \sum_{i-1}^{N} \left(y_i - \beta_0 - \sum_{j-1}^{p} x_{ij}\beta_j \right)^2 \; subject\ to \sum_{j-1}^{p} |\beta_j| \le t \quad (4)$$

where.

arg $\min_\beta$ represents the β vector having minimum MSE.

N denotes number of observations

xij represents data

Ij denotes the vector of p at observation

vi represents the observation i response

p is a vector

β0 and βj denotes scalar parameter

βlasso is estimated coefficient.

General advantage of Lasso can be described as automatic selection of significant features and producing less non-zero coefficient (β values) by discarding others through iterative approach significantly. Compared with the conventional algorithms based on PLS-DA and PCA-LDA, Lasso-PLS-DA can greatly improve the diagnosis efficiency. Use of Lasso PLS-DA algorithm for blood plasma Raman analysis showed significant

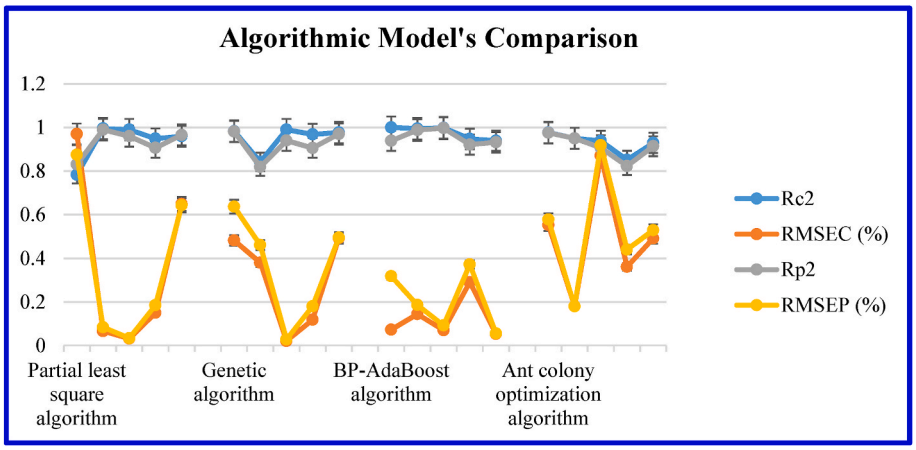

Fig. 19. Comparative map of different algorithmic models with success rate.

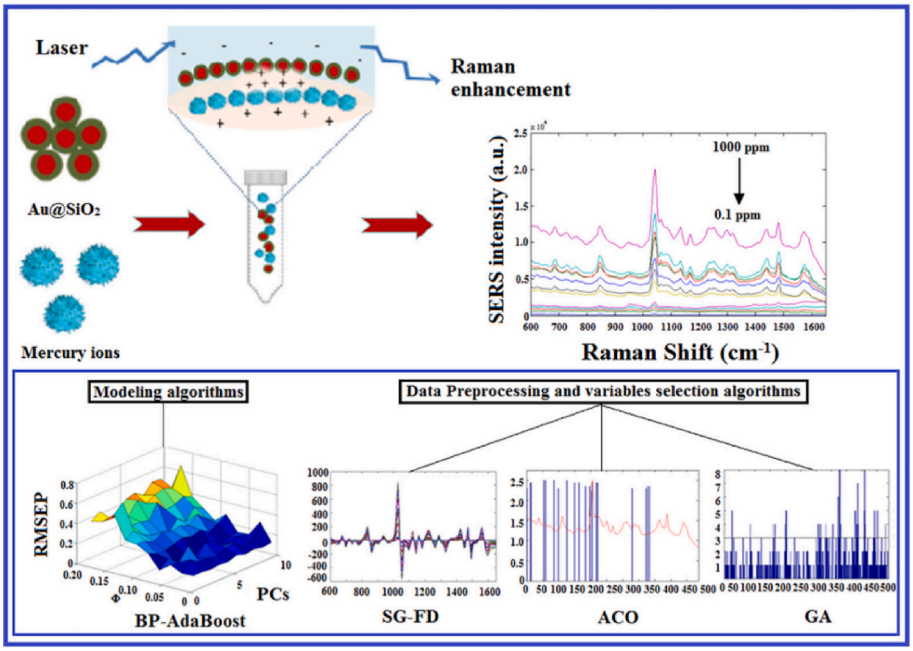

Fig. 20. Illustrative diagram of Raman system with combination of algorithmic calibration models [216].

potential in clinical test especially in classification of different tumor stages. In a study of 160 blood plasma samples taken from 60 normal, 25 treatment 1 (T1) and 75 T2-T4 staged cancer patients results showed that the diagnostic sensitivity of T2–T4 patients separating from T1 patients was 68%, and the specificity was 84.0%. Compared with previous work, the diagnostic specificity was enhanced by 20% by integration of algorithms with Raman spectra (Fig. 22) [219].

Raman chips can be utilized for prior detection of diseases from biomarkers collected from liquid or tissue biopsy. Simultaneously to enhance the Raman signal and distribute the EF on the surface of the sample, an iterative and "learning" design procedure is needed for the geometric structure of nano-scale metal features to maximize the EF and its area at the same time. GA were evolved accompanied with finite difference time domain (FDTD) modeling to optimize the geometry of gold NS on glass slides to use as Raman active surfaces to enhance SERS spectrum.

GA is one of the evolutionary algorithms which evolved from Darwin's theory of evolution. GA imitates procedure of natural selection in order to find the fittest offspring (i.e. SERS metal geometry that gives the highest EF). The workflow of the algorithm is shown in Fig. 23. Genetic algorithm is composed of five main parts: initial population, fitness function, selection, crossover and mutation. Initial population (i.e. geometries) is a set of population which is one of the solutions of the defined problem. Initial population could be randomly generated or predefined. Most important part of the GA is choosing the fitness function which determines the probability of the selection of individuals. The selection of best individuals could be done with different selection algorithms. After the selection process, every parental pair crosses from point of crossover which is selected randomly among genes. Geometry was iterated to reach the optimal design until the fitness score does not increase by more than 10^{-6}. Another important mechanism of the GA is elitism, which describes directly transfer the individuals with the highest fitness value without crossing or mutating. It assures that the best individuals of previous cycle is retained for the next generation.

Binary-coded GA is used for the topology optimization of substrate. Substrate is designed for two different objectives using different fitness functions which were selected as the hot-spot and average EF for the SERS optimization. The enhancement can be increased up to about 10^{17} for hot-spots and 10^{15} levels for averaged enhancements. The resulting structures could be used for label-free single-cell SERS detection. This

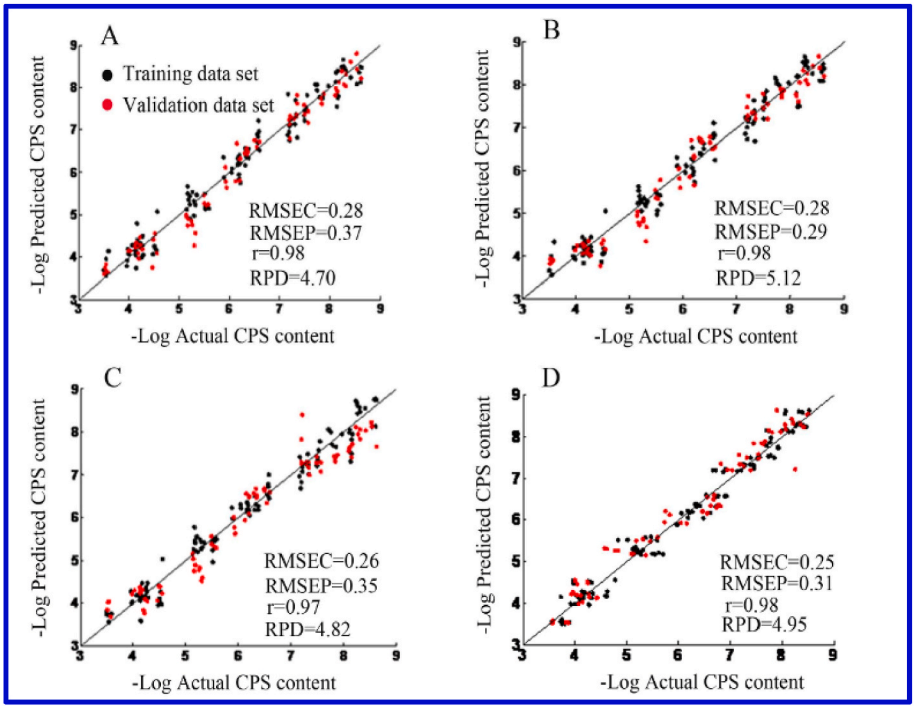

Fig. 21. Linear regression graphs of GC-MS reference values and SERS predicted values of training and validation data sets were compared in different quantification models with linear regression: (A) PLS model, (B) GA-PLS model, (C) siPLS model, (D) siPLS-GA quantification model with SNV data [218].

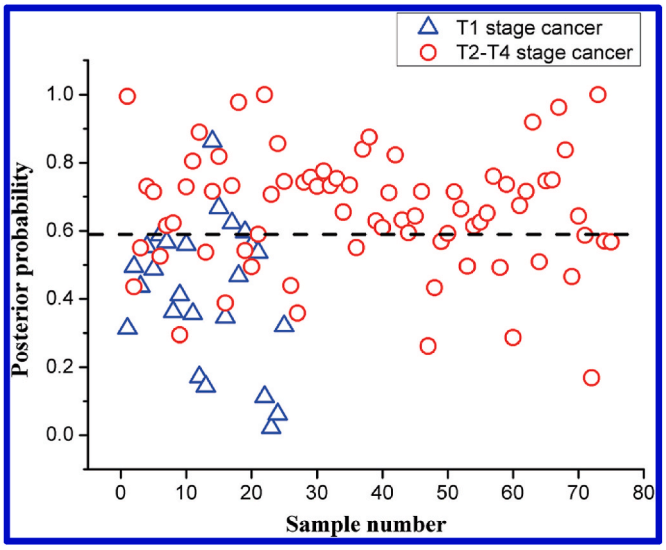

Fig. 22. Used Lasso-PLS-DA to carry out leave-one-out cross-validation of scatter plots of posterior probability values of different stages of cancer. A separate line distinguished T2–T4 stage from T1 stage cancer, with a diagnostic sensitivity of 68% (51/75) and a specificity of 84.0% (21/25) [219].

method converges rapidly and enables multi-objective optimization of photonic materials, metasurface and devices that could take prohibitively long time and large memory by parametric sweeps or random trials and errors [220].

4.2. Microfluidics based SERS measurement

The hospitals occur to have pathogens resistant to antibodies by the time, needed to develop a system to sense bacteria. The system shouldn't needed sample enhancement via orthodox techniques like cell culturing which may be deliberately laborious and time taking. In order to meet this demand, researchers designed an optofluidic SERS detection platform, which utilizes a hollow-core photonic crystal fiber driven by microfluidics and combines it with Ag-NPs to greatly enhance the Raman signals. Comparing with conventional analysis, microfluidic analysis can impressively reduce the magnitude of Raman signals variation by about 50%. Annexation of machine learning algorithm i.e. genetic support vector with microfluidic system can perform automatic counts of cells which is far more enthusiastic than quantitative polymerase chain reaction and many biosensing approaches.

Considering above considerations an optofluidic device was fabricated with multiple time regeneration ability having specificity and detection up to lowest level of 4 colony-forming unit per milliliter (CFU/ml) within 15 min for planktonic bacteria. Moreover, machine learning algorithms further defined the Raman spectrum variances among different strains of bacteria in serum thus found the system much better than many existing biosensing techniques.

Assemblage of optofluidic device: A microfluidic device made up of polydimethylsiloxane (PDMS) was developed with 24 × 14 × 3.5 mm dimensions. Replica modeling was used to regenerate the device multiple time. The master mold was composed of microchannel features made of SU8 photoresist and spin-coated on a 4-inch silicon wafer. The microchannel consisted a length of 12.6 mm and a rectangular cross section of 100 × 60 μm^2 (width, height). The PDMS used to produce the microchannel was mixed at a base/curing agent ratio (w/w) of 10:1, and then degassed in a vacuum for 45 min then cured at 70 °C for 2 h. Punched two 0.75 mm holes at the end of the microchannel to interface with a polytetrafluoroethylene (PTFE) tube. After punching, used 50 W air plasma to permanently bond PDMS to a 75 × 25 × 1.0 mm microscope slide for 30 s. To complete the bonding, the device was placed overnight at 70 °C.

After manufacturing the microfluidic device, channels were combined with hollow-core photonic crystal fiber (HC-PCF) to develop an optofluidic device. Among two microfluidic channels HC-PCF was bridged and attached with epoxy resin. Finally, rinsed the device with DI water and prepared to integrate it into optical system. Adding Ag-NPs to the system greatly enhanced the Raman scattering field, which is

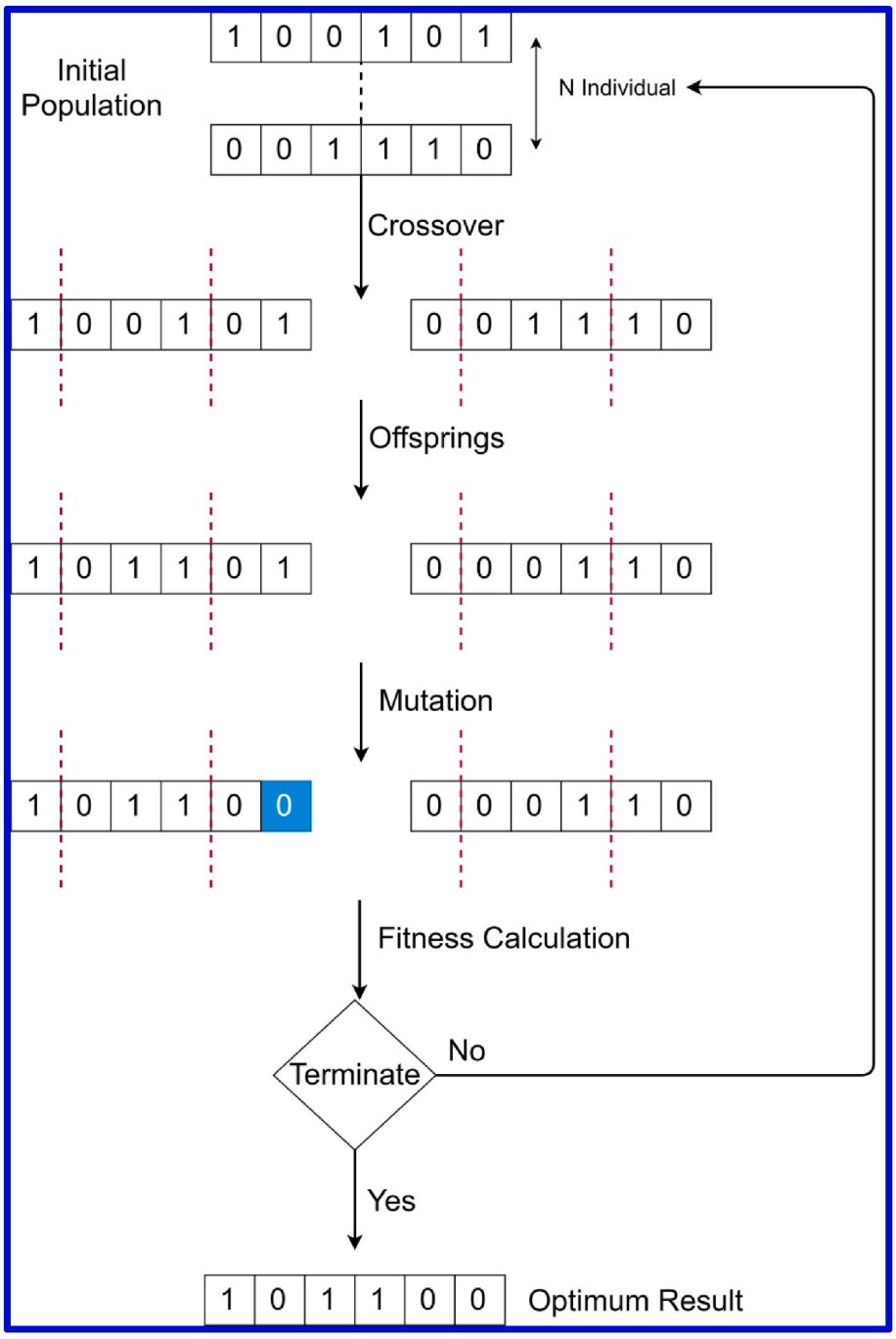

Fig. 23. GA workflow. Evaluated randomly generated individuals to find the most suitable individual. Individuals who survived the fittest crossed with each other, while some genes were mutated. Iteration continued until stall limits have been reached [220].

beneficial to measure the spectra of biomolecules that tend to have low Raman cross-sections (Fig. 24) [221].

The LOD of the system reached the lowest as 4 CFU/mL, which should be lower for some healthcare associated infections. However, this platform presented a valuable pathway in many clinical disciplines in a rapid point-of-care system [221]. Yet to overcome the specificity challenge especially for liquid biopsy and early disease diagnosis, a microfluidic chip containing Raman active protein biomarkers was designed and accompanied with KNN and classification tree machine learning algorithms. CA19-9, HE4, MUC4, MMP7, and mesothelin biomarkers significantly enhanced the reproducibility, prediction accuracy and specificity of Raman active liquid biopsy diagnosis [222].

Microfluidics technology is becoming an efficient tool for various chemical and biological studies. Sedimentation of NPs aggregates on the channel surface can cause a "memory effect", which affects sensitivity and reproducibility. To solve this problem, a new research been presented based on the new SERS calibration free microfluidic paper device (μPAD) consisted of multiple reaction zones. It can simultaneously quantitatively detect multiple cardiac biomarkers-GPBB, CK-MB and cTnT for early diagnosis and prognosis acute myocardial infarction (AMI). Three different Raman probes were produced and then conjugated with their respective detection antibodies, and used as SERS nanotags for cardiac biomarker detection. To quantify cardiac biomarkers level precisely a PLS prediction model was incorporated into the immunosensing system. When the conventional calibration curve cannot accurately estimate cardiac biomarkers, especially in the low and

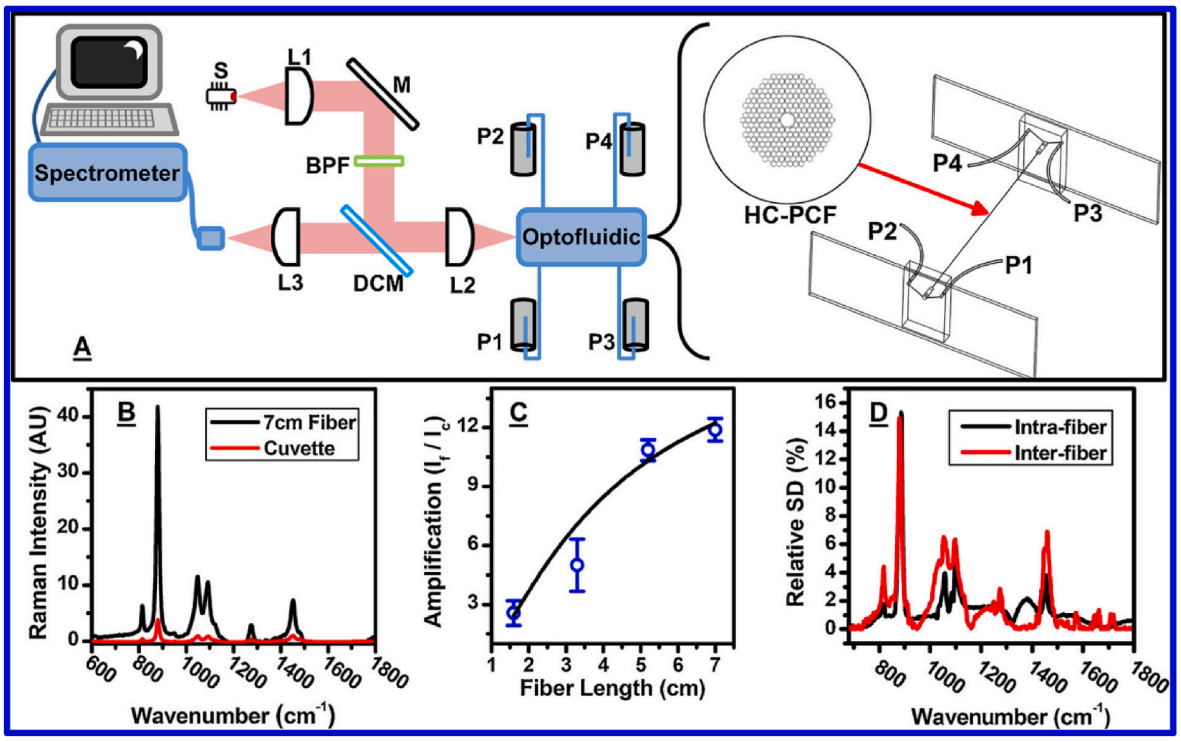

Fig. 24. Summary of overall performance results of the SERS optofluidic device (A) Drawing of optofluidic system accompanied with microfluidic and HC-PCF. S denotes the 785 nm laser, gradient index (GRIN) lens is presented with L1, plano-convex lenses with NA = 0.65 and 0.3 respectively are denoted with L2 and L3, M is an adjustable lens. BPF represents laser line bandpass filter, and DCM as long Distance dichroic mirror, P1-4 are the pressure sources attached to the optical fluid platform, which can push the fluid from the reservoir into the system (B) SERS spectrum of ethanol in cuvette and a 7 cm piece of HC-PCF (C) The relationship between the ratio of fiber strength to cuvette strength and fiber length, the black line is the index best fit (D) Relative SD of Raman spectra measured from 12 filling/rinsing cycles (intra-fiber deviation) and four different fibers (inter-fiber deviation) [221].

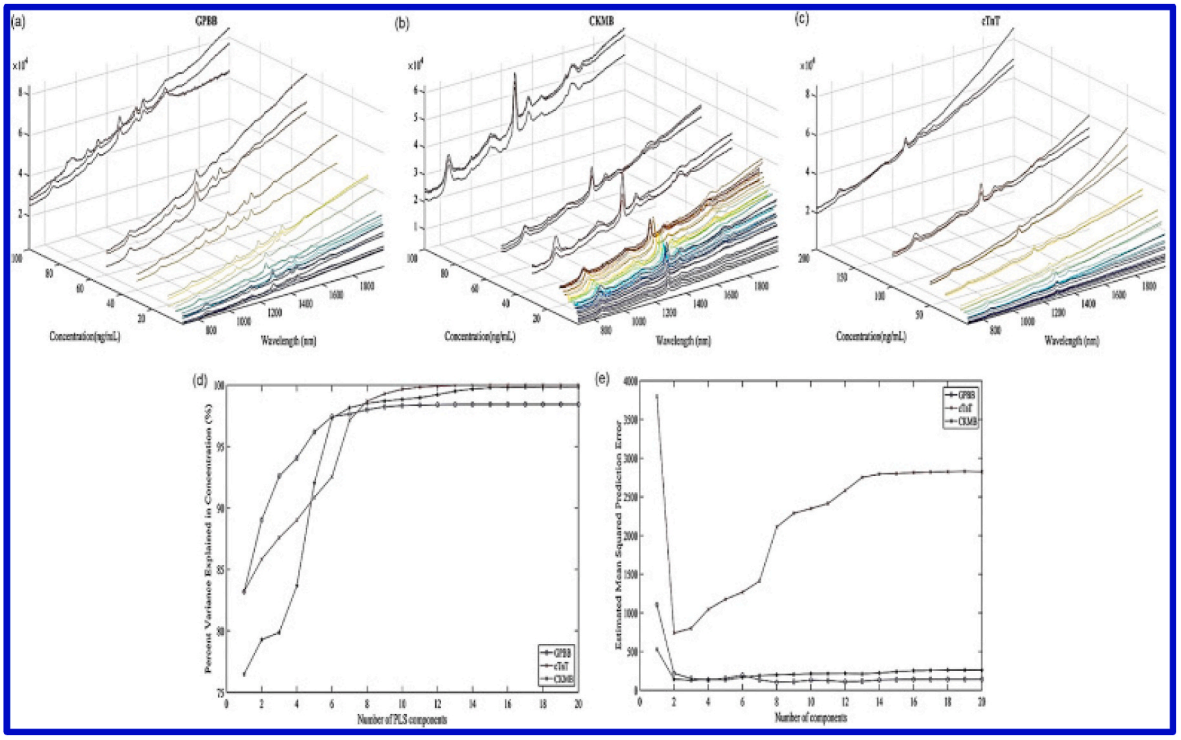

Fig. 25. SERS data of three cardiac biomarkers (700-2000 cm-1) (a) GPBB (conc. 0.001–100 ng mL-1), (b) CK-MB (conc. 0.001–100 ng mL-1) (c) cTnT (conc. 0.001–200 ng mL-1) (d) The percentage difference in the concentration of the three cardiac biomarkers in the first 20 PLS components (e) Estimated RMSEP of the three cardiac biomarkers in first 20 PLS components [225].

high concentration range, this method can be used for absolute quantitative measurement.

An SERS and microfluidic cartridge system was developed to detect sulfamethoxazole within the nanomolar range in an aqueous media. This microfluidic cartridge system was comprised of three fundamental integrant, surface substrate, channel structure and optical window. Electric pump system was used to combine the SERS and cartridge system with already determined flow rate. That ultimately produced stabled and reproducible results with LOD of 2.2×10^{-9} mol/L [223]. To avoid the fungicides treatments in plants and for multiplexed detection and distinguishing the fungus in plants, a microfluidic device was developed. Jasmonic acid, salicylic acid and azelaic acid were three plant hormones which were determined simultaneously within less than 7 min. Moreover, with combination of GA-PLS, CARS-PLS and ACO-PLS algorithms the LOD for jasmonic acid was observed as 4.4 nM, 15 μM for salicylic acid and 10 μM for azelaic acid with reproducible and stable results [224].

Under optimized conditions, the LOD of Raman-based μPAD for GPBB, CK-MB and cTnT was determined to be 8, 10, and 1 $pgmL^{-1}$, respectively, which are far below the clinical cut-off value. On the other hand detection ranges of GPBB, CK-MB and cTnT were 0.01–100, 0.01–100 and 0.001–200 $ngmL^{-1}$, respectively to colorimetric μPAD using bare NPs, covered clinical range of various biomarkers (Fig. 25). In short, this new Raman based μPAD technique when combined with predictive models for biomarker quantification can immensely enhance the reproducibility and sensitivity of microfluidic system [225].

An overview of SERS applications with enhanced specifications are described in Table 1.

Table 1
The review summary of SERS detection applications emphasized with specifications described.

Methods	Detection range	LOD	Properties	References
Fast solid-phase extraction with portable Raman using Au colloidal NPs substrate	0.1–5 μg mL^{-1}	0.04 μg g^{-1}	• Rapidly tracing analysis • Large-scale on-site detection • Complex matrix and different extraction methods	[182]
Ligands bound Ag-NP on silica NPs	10^{-4} – 10^{-7} M	10^{-7} M	• Sensitive and selective detection • Labor extensive	[184]
Ehrlich-reaction using Au-NPs hotspots	14.8–181 ng g^{-1}	2.0 nM	• Accuracy and stability • Low detection limit	[146]
Synergistic effect and plasmonic NPs through SERS	1 mM–0.1 μM	1 nM	• Labor-intensive • Low detection limit	[200]
Synthesized ligand mounted on plasmonic AuNPs	5×10^{-8} – 7.87×10^{-6} M	3.5×10^{-8} M	• Identification effectively • Low detection limit	[212]
Optofluidic label-free SERS platform	3.2–4.3 CFU^{-1} mL	4 CFU^{-1} mL	• Accuracy and stability • Wide detection ranges	[221]
SERS-based microfluidic paper-based device	0.01–100, 0.01–100 and 0.001–200 ng mL^{-1}	8, 10 and 1 pg mL^{-1}	• Identification effectively • High detection limit	[225]

5. Conclusions and future perspective

SERS technology is becoming more and more popular and can be used for accurate and specific identification of chemical or microbial molecules. The combination of SERS and microfluidic devices proves that this research field is currently of high important. SERS measurement has been greatly improved, because the process could be carried out on a large scale in the laboratory and was prone to human error can now be carried out in nanoliter volumes in an automated manner. While, microfluidic platforms require an analytical method capable of detecting in a small volume, so SERS is very suitable for this task. Combination of SERS and algorithmic models reduce the large data sets of variables into small data sets from SERS spectrum. This combinations helps to detect analytes and express the unique fingerprints at molecular level. For biologists and analytical chemists, the quantitative analysis of plant hormones is still very difficult because the endogenous levels of each plant hormone are very low. For researchers, it is a challenge to enrich these low-content natural compounds from plant extracts in the presence of large amounts of interfering substances. In addition, the limited number of plant tissues available for hormone quantification is another challenge.

Current review has covered the aspect of the latest developments and advances in SERS, and also summarized the principles and methods of the Raman system. Moreover, their application in the rapid analysis of plant hormones and the challenges brought by them are explained through the experimental conditions and the SERS spectrum. The novel aspect of this manuscript covers the significance that laser technology possesses as an advantage in the form of fast and reproducible detection ability over old detection methods for plant hormones. Futuristic point of view of SERS studies can lead to the development of more precise and accurate testing and analysis methods. Moreover, development of on-site rapid SERS detection techniques will further provide this technique a space to flourish significantly in common market.

Contribution statement

Syed Muhammad Zaigham Abbas Naqvi: prepared and presented the work, writing- original draft. **Yanyan Zhang:** provided the study materials and maintained the research data. **Shakeel Ahmed:** reviewing and editing. **Abdulraheem Mukhtar Iderawumi:** management activities to annotate and reproducibility of research outputs. **Jiandong Hu:** supervision and conceptualization. **Muhammad Naveed Tahir:** project administration. **Vijaya Raghavan:** project administration.

Declaration of competing interest

The authors declare that they have no known competing financial interests or personal relationships that could have appeared to influence the work reported in this paper.

Acknowledgments

The authors are thankful to the National Natural Science Foundation of China (grant number 32071890, 31671581).

References

[1] A. Santner, M. Estelle, Recent advances and emerging trends in plant hormone signalling, Nature 459 (7250) (2009) 1071–1078.
[2] V. Verma, P. Ravindran, P.P. Kumar, Plant hormone-mediated regulation of stress responses, BMC Plant Biol. 16 (1) (2016) 86.
[3] J. Calleja-Cabrera, M. Boter, L. Oñate-Sánchez, M. Pernas, Root growth adaptation to climate change in crops, Front. Plant Sci. 11 (2020) 544, 544.
[4] P.J. Davies, Plant Hormones: Biosynthesis, Signal Transduction, Action!, Springer Science & Business Media, 2004.
[5] S. Porfírio, R. Sonon, M.D.R. Gomes da Silva, A. Peixe, M.J. Cabrita, P. Azadi, Quantification of free auxins in semi-hardwood plant cuttings and microshoots by dispersive liquid–liquid microextraction/microwave derivatization and GC/MS analysis, Analytical Methods 8 (31) (2016) 6089–6098.
[6] A.G. Pradko, R.P. Litvinovskaya, A.L. Sauchuk, S.V. Drach, A.V. Baranovsky, V. N. Zhabinskii, T.V. Mirantsova, V.A. Khripach, A new ELISA for quantification of brassinosteroids in plants, Steroids 97 (2015) 78–86.

[7] R. Bosco, E. Daeseleire, E. Van Pamel, V. Scariot, L. Leus, Development of an ultrahigh-performance liquid chromatography–electrospray ionization–tandem mass spectrometry method for the simultaneous determination of salicylic acid, jasmonic acid, and abscisic acid in rose leaves, J. Agric. Food Chem. 62 (27) (2014) 6278–6284.
[8] X.-Y. Song, W. Ha, J. Chen, Y.-P. Shi, Application of β-cyclodextrin-modified, carbon nanotube-reinforced hollow fiber to solid-phase microextraction of plant hormones, J. Chromatogr. A 1374 (2014) 23–30.
[9] L. Ge, C.Y.C. Peh, J.W.H. Yong, S.N. Tan, L. Hua, E.S. Ong, Analyses of gibberellins by capillary electrophoresis–mass spectrometry combined with solid-phase extraction, J. Chromatogr. A 1159 (1) (2007) 242–249.
[10] C.J. Anagnostopoulos, K. Liapis, S. Haroutounian, E. Paspatis, Simultaneous determination of different classes of plant growth regulator in high water content agricultural products by liquid chromatography tandem mass spectrometry and time of flight mass spectrometry, J. Liq. Chromatogr. Relat. Technol. 36 (3) (2013) 315–335.
[11] M. Procházka, Surface-enhanced Raman Spectroscopy, Springer International Publishing AG Switzerland, 2016.
[12] J. Jenčo, L.K. Krčmová, D. Solichová, P. Solich, Recent trends in determination of thiamine and its derivatives in clinical practice, J. Chromatogr. A 1510 (2017) 1–12.
[13] P.Q. Tranchida, L. Mondello, Hyphenations of Capillary Chromatography with Mass Spectrometry, Elsevier Science, 2019.
[14] S.C. McGrath, J.R. Deeds, in: Determination of Saxitoxin and Tetrodotoxin in Fish, Analysis of Food Toxins and Toxicants, Wiley, 2017, pp. 403–430.
[15] T. Yoshida, A. Christmann, K. Yamaguchi-Shinozaki, E. Grill, A.R. Fernie, Revisiting the basal role of ABA – roles outside of stress, Trends Plant Sci. 24 (7) (2019) 625–635.
[16] C. Krafft, J. Popp, The many facets of Raman spectroscopy for biomedical analysis, Anal. Bioanal. Chem. 407 (3) (2015) 699–717.
[17] M.A. Tahir, N.E. Dina, H. Cheng, V.K. Valev, L. Zhang, Surface-enhanced Raman spectroscopy for bioanalysis and diagnosis, Nanoscale 13 (27) (2021) 11593–11634.
[18] L.-B. Zhong, Q. Liu, P. Wu, Q.-F. Niu, H. Zhang, Y.-M. Zheng, Facile on-site aqueous pollutant monitoring using a flexible, ultralight, and robust surface-enhanced Raman spectroscopy substrate: interface self-assembly of Au@Ag nanocubes on a polyvinyl chloride template, Environ. Sci. Technol. 52 (10) (2018) 5812–5820.
[19] X. Xie, H. Pu, D.-W. Sun, Recent advances in nanofabrication techniques for SERS substrates and their applications in food safety analysis, Crit. Rev. Food Sci. Nutr. 58 (16) (2018) 2800–2813.
[20] A.M. Dana Cialla-May, Jurgen Popp, in: Surface-Enhanced Raman Spectroscopy, Encyclopedia of Microfluidics and Nanofluidics, 2014, pp. 1–9.
[21] S.A. Ogundare, W.E. van Zyl, in: A Review of Cellulose-Based Substrates for SERS: Fundamentals, Design Principles, Applications, Cellulose, 2019, pp. 1–40.
[22] K.-M. Lee, T.J. Herrman, Determination and prediction of fumonisin contamination in maize by surface–enhanced Raman spectroscopy (SERS), Food Bioprocess Technol. 9 (4) (2016) 588–603.
[23] Y. He, Y. Wang, X. Yang, S. Xie, R. Yuan, Y. Chai, Metal organic frameworks combining CoFe2O4 magnetic nanoparticles as highly efficient SERS sensing platform for ultrasensitive detection of N-terminal pro-brain natriuretic peptide, ACS Appl. Mater. Interfaces 8 (12) (2016) 7683–7690.
[24] S. Ganesh, K. Venkatakrishnan, B. Tan, Quantum scale organic semiconductors for SERS detection of DNA methylation and gene expression, Nat. Commun. 11 (1) (2020) 1135.
[25] G. Schmidl, J. Dellith, H. Schneidewind, D. Zopf, O. Stranik, A. Gawlik, S. Anders, V. Tympel, C. Katzer, F. Schmidl, Formation and characterization of silver nanoparticles embedded in optical transparent materials for plasmonic sensor surfaces, Mater. Sci. Eng., B 193 (2015) 207–216.
[26] S. Su, J. Li, G.C. Lee, K. Sugden, D. Webb, H. Ye, Femtosecond laser-induced microstructures on diamond for microfluidic sensing device applications, Appl. Phys. Lett. 102 (23) (2013) 231913.
[27] L. Yang, J. Wei, Z. Ma, P. Song, J. Ma, Y. Zhao, Z. Huang, M. Zhang, F. Yang, X. Wang, The fabrication of micro/nano structures by laser machining, Nanomaterials 9 (12) (2019) 1789.
[28] R.A. Alvarez-Puebla, D.J. Ross, G.-A. Nazri, R.F. Aroca, Surface-enhanced Raman scattering on nanoshells with tunable surface plasmon resonance, Langmuir 21 (23) (2005) 10504–10508.
[29] J. Chalmers, P. Griffiths, Handbook of Vibrational Spectroscopy, 5 Volumes Set, Wiley, U.K. Chichester, 2002.
[30] S.-Y. Ding, J. Yi, J.-F. Li, B. Ren, D.-Y. Wu, R. Panneerselvam, Z.-Q. Tian, Nanostructure-based plasmon-enhanced Raman spectroscopy for surface analysis of materials, Nature Reviews Materials 1 (6) (2016) 16021.
[31] L.K. Khorashad, L.V. Besteiro, Z. Wang, J. Valentine, A.O. Govorov, Localization of Temperature Using Plasmonic Hot Spots in Metal Nanostructures: the Nano-Optical Antenna Approach and Fano Effect, 2016 arXiv preprint arXiv: 1604.03585.
[32] T.Y. Jeon, D.J. Kim, S.-G. Park, S.-H. Kim, D.-H. Kim, Nanostructured plasmonic substrates for use as SERS sensors, Nano Convergence 3 (1) (2016) 18.
[33] A.M. Alkilany, S.E. Lohse, C.J. Murphy, The gold standard: gold nanoparticle libraries to understand the nano–bio interface, Acc. Chem. Res. 46 (3) (2012) 650–661.
[34] J. Taylor, A. Huefner, L. Li, J. Wingfield, S. Mahajan, Nanoparticles and intracellular applications of surface-enhanced Raman spectroscopy, Analyst 141 (17) (2016) 5037–5055.
[35] P. Zuo, L. Jiang, X. Li, B. Li, P. Ran, X. Li, L. Qu, Y. Lu, Metal (Ag, Pt)–MoS2 hybrids greenly prepared through photochemical reduction of femtosecond laser pulses for SERS and HER, ACS Sustain. Chem. Eng. 6 (6) (2018) 7704–7714.
[36] A.K. Singh, S.A. Khan, Z. Fan, T. Demeritte, D. Senapati, R. Kanchanapally, P. C. Ray, Development of a long-range surface-enhanced Raman spectroscopy ruler, J. Am. Chem. Soc. 134 (20) (2012) 8662–8669.
[37] M. Macias-Montero, R.J. Peláez, V.J. Rico, Z. Saghi, P. Midgley, C.N. Afonso, A. R. González-Elipe, A. Borras, Laser treatment of Ag@ZnO nanorods as long-life-span SERS surfaces, ACS Appl. Mater. Interfaces 7 (4) (2015) 2331–2339.
[38] V. Saikiran, M.H. Dar, R. Kuladeep, N.R. Desai, Ultrafast laser induced subwavelength periodic surface structures on semiconductors/metals and application to SERS studies, MRS Advances 1 (49) (2016) 3317–3327.
[39] E. Polwart, R.L. Keir, C.M. Davidson, W.E. Smith, D.A. Sadler, Novel SERS-active optical fibers prepared by the immobilization of silver colloidal particles, Appl. Spectrosc. 54 (4) (2000) 522–527.
[40] J. Cejkova, V. Prokopec, S. Brazdova, A. Kokaislova, P. Matejka, F. Stepanek, Characterization of copper SERS-active substrates prepared by electrochemical deposition, Appl. Surf. Sci. 255 (18) (2009) 7864–7870.
[41] H.-Y. Hsueh, H.-Y. Chen, Y.-C. Ling, W.-S. Huang, Y.-C. Hung, S. Gwo, R.-M. Ho, A polymer-based SERS-active substrate with gyroid-structured gold multibranches, J. Mater. Chem. C 2 (23) (2014) 4667–4675.
[42] M.E. Koleva, N.N. Nedyalkov, P.A. Atanasov, J.W. Gerlach, D. Hirsch, A. Prager, B. Rauschenbach, N. Fukata, W. Jevasuwan, Porous plasmonic nanocomposites for SERS substrates fabricated by two-step laser method, J. Alloys Compd. 665 (2016) 282–287.
[43] J. Kim, Y. Jang, N.-J. Kim, H. Kim, G.-C. Yi, Y. Shin, M.H. Kim, S. Yoon, Study of chemical enhancement mechanism in non-plasmonic surface enhanced Raman spectroscopy (SERS), Frontiers in Chemistry 7 (582) (2019).
[44] M. Moskovits, Persistent misconceptions regarding SERS, Phys. Chem. Chem. Phys. 15 (15) (2013) 5301–5311.
[45] A. Otto, The 'chemical' (electronic) contribution to surface-enhanced Raman scattering, J. Raman Spectrosc. 36 (6–7) (2005) 497–509.
[46] C. Boerigter, U. Aslam, S. Linic, Mechanism of charge transfer from plasmonic nanostructures to chemically attached materials, ACS Nano 10 (6) (2016) 6108–6115.
[47] K. Kneipp, Chemical contribution to SERS enhancement: an experimental study on a series of polymethine dyes on silver nanoaggregates, J. Phys. Chem. C 120 (37) (2016) 21076–21081.
[48] S.-Y. Ding, E.-M. You, Z.-Q. Tian, M. Moskovits, Electromagnetic theories of surface-enhanced Raman spectroscopy, Chem. Soc. Rev. 46 (13) (2017) 4042–4076.
[49] C.V. Raman, K.S. Krishnan, A new type of secondary radiation, Nature 121 (3048) (1928) 501–502.
[50] X.-S. Zheng, I.J. Jahn, K. Weber, D. Cialla-May, J. Popp, Label-free SERS in biological and biomedical applications: recent progress, current challenges and opportunities, Spectrochim. Acta Mol. Biomol. Spectrosc. 197 (2018) 56–77.
[51] E. Lenzi, D. Jimenez de Aberasturi, L.M. Liz-Marzán, Surface-enhanced Raman scattering tags for three-dimensional bioimaging and biomarker detection, ACS Sens. 4 (5) (2019) 1126–1137.
[52] H. Xu, E.J. Bjerneld, M. Käll, L. Börjesson, Spectroscopy of single hemoglobin molecules by surface enhanced Raman scattering, Phys. Rev. Lett. 83 (21) (1999) 4357–4360.
[53] H. Xu, J. Aizpurua, M. Käll, P. Apell, Electromagnetic contributions to single-molecule sensitivity in surface-enhanced Raman scattering, Phys. Rev. 62 (3) (2000) 4318–4324.
[54] M. Kahraman, E.R. Mullen, A. Korkmaz, S. Wachsmann-Hogiu, Fundamentals and applications of SERS-based bioanalytical sensing, Nanophotonics 6 (5) (2017) 831–852.
[55] P.C. Lee, D. Meisel, Adsorption and surface-enhanced Raman of dyes on silver and gold sols, J. Phys. Chem. 86 (17) (1982) 3391–3395.
[56] A. Campion, P. Kambhampati, Surface-enhanced Raman scattering, Chem. Soc. Rev. 27 (4) (1998) 241–250.
[57] M.E. Stewart, C.R. Anderton, L.B. Thompson, J. Maria, S.K. Gray, J.A. Rogers, R. G. Nuzzo, Nanostructured plasmonic sensors, Chem. Rev. 108 (2) (2008) 494–521.
[58] L. Du, D. Tang, G. Yuan, S. Wei, X. Yuan, Emission pattern of surface-enhanced Raman scattering from single nanoparticle-film junction, Appl. Phys. Lett. 102 (8) (2013), 081117.
[59] N. Guillot, M.L. de la Chapelle, The electromagnetic effect in surface enhanced Raman scattering: enhancement optimization using precisely controlled nanostructures, J. Quant. Spectrosc. Radiat. Transf. 113 (18) (2012) 2321–2333.
[60] L. Billot, M. Lamy de la Chapelle, A.S. Grimault, A. Vial, D. Barchiesi, J.L. Bijeon, P.M. Adam, P. Royer, Surface enhanced Raman scattering on gold nanowire arrays: evidence of strong multipolar surface plasmon resonance enhancement, Chem. Phys. Lett. 422 (4) (2006) 303–307.
[61] J. Prinz, C. Heck, L. Ellerik, V. Merk, I. Bald, DNA origami based Au–Ag-core–shell nanoparticle dimers with single-molecule SERS sensitivity, Nanoscale 8 (10) (2016) 5612–5620.
[62] M. Moskovits, Surface roughness and the enhanced intensity of Raman scattering by molecules adsorbed on metals, J. Chem. Phys. 69 (9) (1978) 4159–4161.
[63] D.S. Wang, M. Kerker, Enhanced Raman scattering by molecules adsorbed at the surface of colloidal spheroids, Phys. Rev. B 24 (4) (1981) 1777–1790.
[64] M. Moskovits, Surface-enhanced spectroscopy, Rev. Mod. Phys. 57 (3) (1985) 783–826.
[65] A. Otto, Surface-enhanced Raman scattering: "classical" and "chemical" origins, in: M. Cardona, G. Güntherodt (Eds.), Light Scattering in Solids IV: Electronics

Scattering, Spin Effects, SERS, and Morphic Effects, Springer Berlin Heidelberg, Berlin, Heidelberg, 1984, pp. 289–418.
[66] J. Wessel, Surface-enhanced optical microscopy, JOSA B 2 (9) (1985) 1538–1541.
[67] X. Chen, in: Adsorption of Dye Molecules on Metallic Nanoparticles: Unraveling the Origins of the Modified Spectral Absorption, Chemical and Physical Sciences, Victoria University of Wellington, 2019, pp. 1–60.
[68] B. Ananthoju, R.K. Biroju, W. Theis, R.A.W. Dryfe, Controlled electrodeposition of gold on graphene: maximization of the defect-enhanced Raman scattering response, Small 15 (48) (2019) 1901555.
[69] V.M. Nardo, A. Sinopoli, L. Kabalan, R.C. Ponterio, F. Saija, S. Trusso, SERS and DFT study of indigo adsorbed on silver nanostructured surface, Spectrochim. Acta Mol. Biomol. Spectrosc. 205 (2018) 465–469.
[70] J. Gersten, A. Nitzan, Electromagnetic theory of enhanced Raman scattering by molecules adsorbed on rough surfaces, J. Chem. Phys. 73 (7) (1980) 3023–3037.
[71] H. Metiu, P. Das, The electromagnetic theory of surface enhanced spectroscopy, Annu. Rev. Phys. Chem. 35 (1) (1984) 507–536.
[72] M. Philpott, Theory of surface enhanced Raman scattering: a prospective view, J. Phys. Colloq. 44 (C10) (1983) C10-C295–C10-303.
[73] A. Wokaun, Surface enhancement of optical fields, Mol. Phys. 56 (1) (1985) 1–33.
[74] C.L. Haynes, A.D. McFarland, R.P. Van Duyne, Surface-enhanced Raman spectroscopy, Anal. Chem. 77 (17) (2005) 338 A–346 A.
[75] C.L. Haynes, C.R. Yonzon, X. Zhang, R.P. Van Duyne, Surface-enhanced Raman sensors: early history and the development of sensors for quantitative biowarfare agent and glucose detection, J. Raman Spectrosc. 36 (6–7) (2005) 471–484.
[76] T. Itoh, Y.S. Yamamoto, Recent topics on single-molecule fluctuation analysis using blinking in surface-enhanced resonance Raman scattering: clarification by the electromagnetic mechanism, Analyst 141 (17) (2016) 5000–5009.
[77] J. Olivo, C.J. Zapata-Rodríguez, M. Cuevas, Spatial modulation of the electromagnetic energy transfer by excitation of graphene waveguide surface plasmons, J. Opt. 21 (4) (2019), 045002.
[78] G.C. Schatz, M.A. Young, R.P. Van Duyne, Electromagnetic mechanism of SERS, in: K. Kneipp, M. Moskovits, H. Kneipp (Eds.), Surface-Enhanced Raman Scattering: Physics and Applications, Springer Berlin Heidelberg, Berlin, Heidelberg, 2006, pp. 19–45.
[79] T. Itoh, Frontiers in electromagnetic mechanism of SERS, in: K. Katrin, T. Zhongqun, O. Yukihiro (Eds.), Recent Developments in Plasmon-Supported Raman Spectroscopy: 45 Years of Enhanced Raman Signals, World Scientific, 2017, p. 33.
[80] H. Gao, E. Herrmann, X. Wang, Programmable field localization and enhancement effects on a non-structured planar surface with a permittivity gradient, Opt Express 28 (2) (2020) 1051–1060.
[81] N. Félidj, J. Aubard, G. Lévi, J.R. Krenn, M. Salerno, G. Schider, B. Lamprecht, A. Leitner, F.R. Aussenegg, Controlling the optical response of regular arrays of gold particles for surface-enhanced Raman scattering, Phys. Rev. B 65 (7) (2002), 075419.
[82] N. Zhang, K. Liu, Z. Liu, H. Song, X. Zeng, D. Ji, A. Cheney, S. Jiang, Q. Gan, Ultrabroadband metasurface for efficient light trapping and localization: a universal surface-enhanced Raman spectroscopy substrate for "all" excitation wavelengths, Advanced Materials Interfaces 2 (10) (2015) 1500142.
[83] O. Graniel, I. Iatsunskyi, E. Coy, C. Humbert, G. Barbillon, T. Michel, D. Maurin, S. Balme, P. Miele, M. Bechelany, Au-covered hollow urchin-like ZnO nanostructures for surface-enhanced Raman scattering sensing, J. Mater. Chem. C 7 (47) (2019) 15066–15073.
[84] M. Tavakkoli Yaraki, S. Daqiqeh Rezaei, Y.N. Tan, Simulation guided design of silver nanostructures for plasmon-enhanced fluorescence, singlet oxygen generation and SERS applications, Phys. Chem. Chem. Phys. 22 (10) (2020) 5673–5687.
[85] M. Kahraman, A. Ozbay, H. Yuksel, R. Solmaz, B. Demir, H. Caglayan, Tunable plasmonic silver nanodomes for surface-enhanced Raman scattering, Plasmonics 13 (3) (2018) 785–795.
[86] X. Wang, W. Shi, G. She, L. Mu, Surface-Enhanced Raman Scattering (SERS) on transition metal and semiconductor nanostructures, Phys. Chem. Chem. Phys. 14 (17) (2012) 5891–5901.
[87] I. Alessandri, J.R. Lombardi, Enhanced Raman scattering with dielectrics, Chem. Rev. 116 (24) (2016) 14921–14981.
[88] D.L. Jeanmaire, R.P. Van Duyne, Surface Raman spectroelectrochemistry: Part I. Heterocyclic, aromatic, and aliphatic amines adsorbed on the anodized silver electrode, J. Electroanal. Chem. Interfacial Electrochem. 84 (1) (1977) 1–20.
[89] I. Mrozek, A. Otto, SERS — a long-range effect? Appl. Phys. A 49 (4) (1989) 389–391.
[90] I. Mrozek, A. Otto, Quantitative separation of the "classical" electromagnetic and the "chemical" contribution to surface enhanced Raman scattering, J. Electron. Spectrosc. Relat. Phenom. 54–55 (1990) 895–911.
[91] A.T. Zayak, Y.S. Hu, H. Choo, J. Bokor, S. Cabrini, P.J. Schuck, J.B. Neaton, Chemical Raman enhancement of organic adsorbates on metal surfaces, Phys. Rev. Lett. 106 (8) (2011), 083003.
[92] Y. Liu, Z. Lu, H. Zhu, W. Hasi, Characterization of a chloride-activated surface complex and corresponding enhancement mechanism by SERS saturation effect, J. Phys. Chem. C 121 (1) (2017) 950–957.
[93] E. Le Ru, P. Etchegoin, Principles of Surface-Enhanced Raman Spectroscopy: and Related Plasmonic Effects, Elsevier, 2008.
[94] F.J. Adrian, Charge transfer effects in surface-enhanced Raman scatteringa), J. Chem. Phys. 77 (11) (1982) 5302–5314.
[95] P. Zhai, L. Liu, X. Gu, T. Wang, Y. Gong, Interface engineering for lithium metal anodes in liquid electrolyte, Advanced Energy Materials 10 (34) (2020) 2001257.
[96] M. Ha, J.-H. Kim, M. You, Q. Li, C. Fan, J.-M. Nam, Multicomponent plasmonic nanoparticles: from heterostructured nanoparticles to colloidal composite nanostructures, Chem. Rev. 119 (24) (2019) 12208–12278.
[97] N.L. Wong, Surface-Enhanced Raman Spectroscopy (SERS): Advances in Single Molecule Detection and Elucidating the Chemical Enhancement Mechanism, Field of Chemistry, Northwestern University, 2018.
[98] Y. Liu, D. Yang, Y. Zhao, Y. Yang, S. Wu, J. Wang, L. Xia, P. Song, Solvent-controlled plasmon-assisted surface catalysis reaction of 4-aminothiophenol dimerizing to p,p'-dimercaptoazobenzene on Ag nanoparticles, Heliyon 5 (4) (2019), e01545.
[99] M.A. Delsuc, M. Vitorino, B. Kieffer, Determination of protein structure and dynamics by NMR, in: J.-P. RENAUD (Ed.), Structural Biology in Drug Discovery, 2020, pp. 295–323.
[100] B. Liu, B. Thielert, A. Reutter, R. Stosch, P. Lemmens, Quantifying the contribution of chemical enhancement to SERS: a model based on the analysis of light-induced degradation processes, J. Phys. Chem. C 123 (31) (2019) 19119–19124.
[101] X. Jiang, Y. Chen, J. Du, X. Li, Y. Shen, M. Yang, X. Han, L. Yang, B. Zhao, Comparative study of semiconductor TiO2 and noble metal Ag substrates: the differences between chemical enhancement and electromagnetic enhancement in SERS, J. Raman Spectrosc. 49 (8) (2018) 1257–1264.
[102] Y. Liu, H. Ma, X.X. Han, B. Zhao, Metal–semiconductor heterostructures for surface-enhanced Raman scattering: synergistic contribution of plasmons and charge transfer, Materials Horizons (2021).
[103] S. Thirumalairajan, K. Girija, Efficient and tunable shape selective synthesis of Ag/CeO2 nanostructures modified highly stable SERS substrate for ultrasensitive detection of pesticides on the surface of an apple, Nanoscale Advances 2 (8) (2020) 3570–3581.
[104] A. Shiohara, Y. Wang, L.M. Liz-Marzán, Recent approaches toward creation of hot spots for SERS detection, J. Photochem. Photobiol. C Photochem. Rev. 21 (2014) 2–25.
[105] J.R. Lombardi, R.L. Birke, Time-dependent picture of the charge-transfer contributions to surface enhanced Raman spectroscopy, J. Chem. Phys. 126 (24) (2007) 244709.
[106] J.R. Lombardi, R.L. Birke, The theory of surface-enhanced Raman scattering, J. Chem. Phys. 136 (14) (2012) 144704.
[107] J.R. Lombardi, R.L. Birke, Theory of surface-enhanced Raman scattering in semiconductors, J. Phys. Chem. C 118 (20) (2014) 11120–11130.
[108] J.M. Bello, V.A. Narayanan, D.L. Stokes, T. Vo Dinh, Fiber-optic remote sensor for in situ surface-enhanced Raman scattering analysis, Anal. Chem. 62 (22) (1990) 2437–2441.
[109] J. Prakash, R.A. Harris, H.C. Swart, Embedded plasmonic nanostructures: synthesis, fundamental aspects and their surface enhanced Raman scattering applications, Int. Rev. Phys. Chem. 35 (3) (2016) 353–398.
[110] D. Zhang, P. Liang, Z. Yu, J. Huang, D. Ni, H. Shu, Q.-m. Dong, The effect of solvent environment toward optimization of SERS sensors for pesticides detection from chemical enhancement aspects, Sensor. Actuator. B Chem. 256 (2018) 721–728.
[111] A. Gellé, T. Jin, L. de la Garza, G.D. Price, L.V. Besteiro, A. Moores, Applications of plasmon-enhanced nanocatalysis to organic transformations, Chem. Rev. 120 (2) (2020) 986–1041.
[112] K.H. Lee, in: Double Surface Plasmon Polaritons (SPPs) for Sensing Purposes, School of Materials Science and Engineering, Nanyang Technological University, 2011, p. 166.
[113] M.J. Seo, G.W. Kim, P.V. Tsalu, S.W. Moon, J.W. Ha, Role of chemical interface damping for tuning chemical enhancement in resonance surface-enhanced Raman scattering of plasmonic gold nanorods, Nanoscale Horizons 5 (2) (2020) 345–349.
[114] S. Huh, J. Park, Y.S. Kim, K.S. Kim, B.H. Hong, J.-M. Nam, UV/Ozone-Oxidized large-scale graphene platform with large chemical enhancement in surface-enhanced Raman scattering, ACS Nano 5 (12) (2011) 9799–9806.
[115] G. Kaur, K. Kavitha, I. Lahiri, Transfer-free graphene growth on dielectric substrates: a review of the growth mechanism, Crit. Rev. Solid State Mater. Sci. 44 (2) (2019) 157–209.
[116] P. Ren, E. Pu, D. Liu, Y. Wang, B. Xiang, X. Ren, Fabrication of nitrogen-doped graphenes by pulsed laser deposition and improved chemical enhancement for Raman spectroscopy, Mater. Lett. 204 (2017) 65–68.
[117] R. Rickman, The Development of Tip-Enhanced Raman Spectroscopy for Defect Characterisation in Graphene, Department of Physics, Swansea University (United Kingdom), United Kingdom, 2013.
[118] A. Taguchi, J. Yu, P. Verma, S. Kawata, Optical antennas with multiple plasmonic nanoparticles for tip-enhanced Raman microscopy, Nanoscale 7 (41) (2015) 17424–17433.
[119] P. Verma, Tip-enhanced Raman spectroscopy: technique and recent advances, Chem. Rev. 117 (9) (2017) 6447–6466.
[120] J. Guo, Scanning probe microscopy, in: J. Guo (Ed.), High Resolution Imaging, Spectroscopy and Nuclear Quantum Effects of Interfacial Water, Springer Singapore, Singapore, 2018, pp. 23–41.
[121] K. Edelmann, L. Gerhard, M. Winkler, L. Wilmes, V. Rai, M. Schumann, C. Kern, M. Meyer, M. Wegener, W. Wulfhekel, Light collection from a low-temperature scanning tunneling microscope using integrated mirror tips fabricated by direct laser writing, Rev. Sci. Instrum. 89 (12) (2018) 123107.
[122] W. Chao, B.D. Harteneck, J.A. Liddle, E.H. Anderson, D.T. Attwood, Soft X-ray microscopy at a spatial resolution better than 15 nm, Nature 435 (7046) (2005) 1210–1213.

[123] R. Kato, T. Umakoshi, R.T. Sam, P. Verma, Probing nanoscale defects and wrinkles in MoS2 by tip-enhanced Raman spectroscopic imaging, Appl. Phys. Lett. 114 (7) (2019), 073105.
[124] Z. Jinxin, W. Wei, H.B. Jens, S.-M. Lukas, L. Christoph, G. Petra, Spatial and spectral mode mapping of a dielectric nanodot by broadband interferometric homodyne scanning near-field spectroscopy, Advanced Photonics 2 (4) (2020) 1–11.
[125] G. Binnig, C.F. Quate, C. Gerber, Atomic force microscope, Phys. Rev. Lett. 56 (9) (1986) 930–933.
[126] G. Binnig, H. Rohrer, C. Gerber, E. Weibel, Surface studies by scanning tunneling microscopy, Phys. Rev. Lett. 49 (1) (1982) 57–61.
[127] Z. Zhang, S. Sheng, R. Wang, M. Sun, Tip-enhanced Raman spectroscopy, Anal. Chem. 88 (19) (2016) 9328–9346.
[128] A. Dutta, A. Chattopadhyay, Surface and tip-enhanced Raman spectroscopy at the plasmonic hot spot of a coordination complex-conjugated gold nanoparticle dimer, J. Phys. Chem. C 121 (34) (2017) 18854–18861.
[129] T. Deckert-Gaudig, A. Taguchi, S. Kawata, V. Deckert, Tip-enhanced Raman spectroscopy – from early developments to recent advances, Chem. Soc. Rev. 46 (13) (2017) 4077–4110.
[130] M.S. Anderson, Locally enhanced Raman spectroscopy with an atomic force microscope, Appl. Phys. Lett. 76 (21) (2000) 3130–3132.
[131] B. Pettinger, G. Picardi, R. Schuster, G. Ertl, Surface-enhanced and STM-tip-enhanced Raman spectroscopy at metal surfaces, Single Mol. 3 (5–6) (2002) 285–294.
[132] E.M. van Schrojenstein Lantman, T. Deckert-Gaudig, A.J.G. Mank, V. Deckert, B. M. Weckhuysen, Catalytic processes monitored at the nanoscale with tip-enhanced Raman spectroscopy, Nat. Nanotechnol. 7 (9) (2012) 583–586.
[133] B. Schrader, Infrared and Raman Spectroscopy: Methods and Applications, John Wiley & Sons, 2008.
[134] Z. Zhang, S. Mukamel, Fluorescence spectroscopy of vibronic polaritons of molecular aggregates in optical microcavities, Chem. Phys. Lett. 683 (2017) 653–657.
[135] M. Hashimoto, T. Yuzawa, C. Kato, K. Iwata, H. Hamaguchi, Handbook of Vibrational Spectroscopy, John Wiley & Sons Ltd, Chichester, UK, 2002.
[136] L.A. Leites, S.S. Bukalov, J.E. Mangette, T.A. Schmedake, R. West, Conformational polymorphism of solid tetramesityldisilene Mes2SiSiMes2 (Raman, UV–vis, IR and fluorescence study), Spectrochim. Acta Mol. Biomol. Spectrosc. 59 (9) (2003) 1975–1988.
[137] J.B. Wiester, in: Investigating the Similarities and Differences Among UV/Vis, Infrared, Fluorescence, and Raman Spectroscopies through Discussion of Light–Matter Interactions, Raman Spectroscopy in the Undergraduate Curriculum, American Chemical Society, 2018, pp. 13–33.
[138] B. Pettinger, B. Ren, G. Picardi, R. Schuster, G. Ertl, Nanoscale probing of adsorbed species by tip-enhanced Raman spectroscopy, Phys. Rev. Lett. 92 (9) (2004), 096101.
[139] M.S. Anderson, W.T. Pike, A Raman-atomic force microscope for apertureless-near-field spectroscopy and optical trapping, Rev. Sci. Instrum. 73 (3) (2002) 1198–1203.
[140] G.I.N. Waterhouse, G.A. Bowmaker, J.B. Metson, The thermal decomposition of silver (I, III) oxide: a combined XRD, FT-IR and Raman spectroscopic study, Phys. Chem. Chem. Phys. 3 (17) (2001) 3838–3845.
[141] A. Sabur, M. Havel, Y. Gogotsi, SERS intensity optimization by controlling the size and shape of faceted gold nanoparticles, J. Raman Spectrosc. 39 (1) (2008) 61–67.
[142] S. Schlücker, Surface-enhanced Raman spectroscopy: concepts and chemical applications, Angew. Chem. Int. Ed. 53 (19) (2014) 4756–4795.
[143] M.J. West, M.J. Went, Detection of drugs of abuse by Raman spectroscopy, Drug Test. Anal. 3 (9) (2011) 532–538.
[144] M. Wahadoszamen, A. Rahaman, N.M. Hoque, A.I. Talukder, K.M. Abedin, A. Haider, Laser Raman spectroscopy with different excitation sources and extension to surface enhanced Raman spectroscopy, Journal of Spectroscopy 15 (2015) 1–8.
[145] K. Sornalingam, A. McDonagh, J.L. Zhou, M.A.H. Johir, M.B. Ahmed, Photocatalysis of estrone in water and wastewater: comparison between Au-TiO2 nanocomposite and TiO2, and degradation by-products, Sci. Total Environ. 610–611 (2018) 521–530.
[146] F. Wang, X. Gu, C. Zheng, F. Dong, L. Zhang, Y. Cai, Z. You, J. You, S. Du, Z. Zhang, Ehrlich reaction evoked multiple spectral resonances and gold nanoparticle hotspots for Raman detection of plant hormone, Anal. Chem. 89 (17) (2017) 8836–8843.
[147] Y.D. Suh, J.M. Nam, D.K. Lim, K.S. Jeon, Single Nanoparticle Having a Nanogap between a Core Material and a Shell Material, and Preparation Method Thereof, Korea Research Institute of Chemical Technology KRICT, Seoul National University R&DB Foundation, 2016.
[148] O.G. Rehrauer, in: Multivariate Statistical Methods that Enable Fast Raman Spectroscopy, Chemistry, Purdue University, 2016, pp. 1–123.
[149] F. Joux, P. Lebaron, Use of fluorescent probes to assess physiological functions of bacteriaat single-cell level, Microb. Infect. 2 (12) (2000) 1523–1535.
[150] V.R. Salares, C.R. Eves, P.R. Carey, On the detection of fingerprints by laser excited luminescence, Forensic Sci. Int. 14 (3) (1979) 229–237.
[151] P.K. Jain, X. Huang, I.H. El-Sayed, M.A. El-Sayed, Noble metals on the nanoscale: optical and photothermal properties and some applications in imaging, sensing, biology, and medicine, Acc. Chem. Res. 41 (12) (2008) 1578–1586.
[152] E.-Z. Tan, P.-G. Yin, T.-t. You, H. Wang, L. Guo, Three dimensional design of large-scale TiO2 nanorods scaffold decorated by silver nanoparticles as SERS sensor for ultrasensitive malachite green detection, ACS Appl. Mater. Interfaces 4 (7) (2012) 3432–3437.
[153] M. Moskovits, Surface-enhanced Raman spectroscopy: a brief retrospective, J. Raman Spectrosc. 36 (6–7) (2005) 485–496.
[154] G. Wang, R. Yi, X. Zhai, R. Bian, Y. Gao, D. Cai, J. Liu, X. Huang, G. Lu, H. Li, W. Huang, A flexible SERS-active film for studying the effect of non-metallic nanostructures on Raman enhancement, Nanoscale 10 (35) (2018) 16895–16901.
[155] M.J. Natan, R.D. Freeman, W.E. Doering, M.E. Piotti, Wavelength Selective SERS Nanotags, SICPA Holding SA, 2017.
[156] M. Jacob, Organic Semiconductors, 2015, Shu-Kun Lin, MDPI AG, Basel, Switzerland, 2008.
[157] N.R. Shanmugam, Switch Based Hybrid Sensors, Biomedical Engineering, The University of Texas at Dallas, 2014.
[158] M.J. Natan, R.G. Freeman, W.E. Doering, M.E. Piotti, Wavelength Selective Sers Nanotags, SICPA Holding SA, 2013.
[159] C.H. Foyer, B. Rasool, J.W. Davey, R.D. Hancock, Cross-tolerance to biotic and abiotic stresses in plants: a focus on resistance to aphid infestation, J. Exp. Bot. 67 (7) (2016) 2025–2037.
[160] R.L. Metcalf, W.H. Luckmann, Introduction to Insect Pest Management, 3 ed., John Wiley and Sons, 1994.
[161] C.J. Nelson, L.E. Moser, Plant factors affecting forage quality, in: G.C.F. Jr (Ed.), Forage Quality, Evaluation, and Utilization, 2015, pp. 115–154.
[162] C. Kissoudis, C. van de Wiel, R.G.F. Visser, G. van der Linden, Enhancing crop resilience to combined abiotic and biotic stress through the dissection of physiological and molecular crosstalk, Front. Plant Sci. 5 (2014) 207.
[163] M. Adil, B.R. Jeong, Chapter 31 - role of melatonin and serotonin in plant stress tolerance, in: D.K. Tripathi, V. Pratap Singh, D.K. Chauhan, S. Sharma, S. M. Prasad, N.K. Dubey, N. Ramawat (Eds.), Plant Life under Changing Environment, Academic Press, 2020, pp. 775–791.
[164] J. Zhou, Q. Liu, F. Zhang, Y. Wang, S. Zhang, H. Cheng, L. Yan, L. Li, F. Chen, X. Xie, Overexpression of OsPIL15, a phytochrome-interacting factor-like protein gene, represses etiolated seedling growth in rice, J. Integr. Plant Biol. 56 (4) (2014) 373–387.
[165] S. Du, C. Yu, L. Tang, L. Lu, Applications of SERS in the detection of stress-related substances, Nanomaterials 8 (10) (2018) 757.
[166] Y. Yuan, Y. Lin, B. Gu, N. Panwar, S.C. Tjin, J. Song, J. Qu, K.-T. Yong, Optical trapping-assisted SERS platform for chemical and biosensing applications: design perspectives, Coord. Chem. Rev. 339 (2017) 138–152.
[167] Z. Luo, K. Chen, D. Lu, H. Han, M. Zou, Synthesis of p-aminothiophenol-embedded gold/silver core-shell nanostructures as novel SERS tags for biosensing applications, Microchimica Acta 173 (1) (2011) 149–156.
[168] A.P. Dempster, New methods for reasoning towards posterior distributions based on sample data, Ann. Math. Stat. 37 (2) (1966) 355–374.
[169] A.P. Dempster, Upper and lower probabilities generated by a random closed interval, Ann. Math. Stat. 39 (3) (1968) 957–966.
[170] V. Kaftandjian, Z. Yue Min, O. Dupuis, D. Babot, The combined use of the evidence theory and fuzzy logic for improving multimodal nondestructive testing systems, IEEE Transactions on Instrumentation and Measurement 54 (5) (2005) 1968–1977.
[171] Y.M. Zhu, L. Bentabet, O. Dupuis, V. Kaftandjian, D. Babot, M. Rombaut, Automatic determination of mass functions in Dempster-Shafer theory using fuzzy C-means and spatial neighborhood information for image segmentation, Opt. Eng. 41 (2002) 760–770.
[172] G. Shafer, A Mathematical Theory of Evidence, Princeton university press, 1976.
[173] N. Sghaier, R.B. Ayed, R.B. Marzoug, A. Rebai, Dempster-shafer theory for the prediction of auxin-response elements (AuxREs) in plant genomes, BioMed Res. Int. (2018) 1–13.
[174] P. Blanchard, E. Brüning, Mathematical Methods in Physics: Distributions, Hilbert Space Operators, Variational Methods, and Applications in Quantum Physics, 2 ed., Birkhäuser, 2015.
[175] H. Chermette, Chemical reactivity indexes in density functional theory, J. Comput. Chem. 20 (1) (1999) 129–154.
[176] R.G. Parr, W. Yang, Density-functional theory of the electronic structure of molecules, Annu. Rev. Phys. Chem. 46 (1) (1995) 701–728.
[177] F. Qu, Y. Pan, L. Lin, C. Cai, T. Dong, Y. He, P. Nie, Experimental and theoretical study on terahertz absorption characteristics and spectral de-noising of three plant growth regulators, J. Infrared, Millim. Terahertz Waves 39 (10) (2018) 1015–1027.
[178] N.H. Ly, T.H. Nguyen, N.Đ. Nghi, Y.-H. Kim, S.-W. Joo, Surface-enhanced Raman scattering detection of fipronil pesticide adsorbed on silver nanoparticles, Sensors 19 (6) (2019) 1355.
[179] W. Xiong, P. Ndokoye, M.K.H. Leung, Chapter 2 - noble metal–based nanosensors for environmental detection, in: Q. Zhao (Ed.), Advanced Nanomaterials for Pollutant Sensing and Environmental Catalysis, Elsevier, 2020, pp. 39–78.
[180] H. Lai, F. Xu, L. Wang, A review of the preparation and application of magnetic nanoparticles for surface-enhanced Raman scattering, J. Mater. Sci. 53 (12) (2018) 8677–8698.
[181] X. Wu, J. He, J. Chen, S. Yang, D. Zha, Alleviation of exogenous 6-benzyladenine on two genotypes of eggplant (Solanum melongena Mill.) growth under salt stress, Protoplasma 251 (1) (2014) 169–176.
[182] P. Zhang, L.M. Wang, D.W. Zheng, T.F. Lin, X.D. Wei, X.Y. Liu, H.Q. Wang, Surface-enhanced Raman spectroscopic analysis of N(6)-benzylaminopurine residue quantity in sprouts with gold nanoparticles, J. Environ. Sci. Health Part B Pestic. Food Contam. Agric. Wastes 53 (9) (2018) 561–566.

[183] V. Bugatti, G. Viscusi, C. Naddeo, G. Gorrasi, Nanocomposites based on PCL and halloysite nanotubes filled with lysozyme: effect of draw ratio on the physical properties and release analysis, Nanomaterials 7 (8) (2017) 213.
[184] J.M. Choi, E. Hahm, K. Park, D. Jeong, W.-Y. Rho, J. Kim, D.H. Jeong, Y.-S. Lee, S. H. Jhang, H.J. Chung, E. Cho, J.-H. Yu, B.-H. Jun, S. Jung, SERS-based flavonoid detection using ethylenediamine-β-cyclodextrin as a capturing ligand, Nanomaterials 7 (1) (2017).
[185] M. Chen, Z. Zhang, M. Liu, C. Qiu, H. Yang, X. Chen, In situ fabrication of label-free optical sensing paper strips for the rapid surface-enhanced Raman scattering (SERS) detection of brassinosteroids in plant tissues, Talanta 165 (2017) 313–320.
[186] W. Wei, Q. Huang, Rapid fabrication of silver nanoparticle-coated filter paper as SERS substrate for low-abundance molecules detection, Spectrochim. Acta Mol. Biomol. Spectrosc. 179 (2017) 211–215.
[188] P. Zhang, L. Wang, X. Wei, T. Lin, H. Wang, X. Liu, D. Zheng, Rapid detection of 6-benzylaminopurine residuals using surface-enhanced Raman scattering, J. Appl. Spectrosc. 85 (5) (2018) 880–884.
[189] N.M.B. Perney, J.J. Baumberg, M.E. Zoorob, M.D.B. Charlton, S. Mahnkopf, C. M. Netti, Tuning localized plasmons in nanostructured substrates for surface-enhanced Raman scattering, Opt Express 14 (2) (2006) 847–857.
[190] N.M.B. Perney, F.J. García de Abajo, J.J. Baumberg, A. Tang, M.C. Netti, M.D. B. Charlton, M.E. Zoorob, Tuning localized plasmon cavities for optimized surface-enhanced Raman scattering, Phys. Rev. B 76 (3) (2007), 035426.
[191] C. Netti, J.R. Lincoln, in: Probing Molecules with Photonic Crystal Surface-Enhanced Raman Spectroscopy, Microscopy and Analysis, Wiley Analytical Science, Southampton, UK, 2005, pp. 13–15.
[192] K.C. Vernon, T.J. Davis, F.H. Scholes, D.E. Gómez, D. Lau, Physical mechanisms behind the SERS enhancement of pyramidal pit substrates, J. Raman Spectrosc. 41 (10) (2010) 1106–1111.
[193] P. Gu, Z. Zhou, Z. Zhao, H. Möhwald, C. Li, R.C. Chiechi, Z. Shi, G. Zhang, 3D zig-zag nanogaps based on nanoskiving for plasmonic nanofocusing, Nanoscale 11 (8) (2019) 3583–3590.
[194] X. Li, G. Chen, L. Yang, Z. Jin, J. Liu, Multifunctional Au-coated TiO2 nanotube Arrays as recyclable SERS substrates for multifold organic pollutants detection, Adv. Funct. Mater. 20 (17) (2010) 2815–2824.
[195] E. Umut, Surface modification of nanoparticles used in biomedical applications, Modern Surface Engineering Treatments 20 (2013) 185–208.
[196] J. Chi, X. Zhang, Y. Wang, C. Shao, L. Shang, Y. Zhao, Bio-inspired wettability patterns for biomedical applications, Materials Horizons 8 (1) (2021) 124–144.
[197] L. Shang, Y. Cheng, Y. Zhao, Emerging droplet microfluidics, Chem. Rev. 117 (12) (2017) 7964–8040.
[198] Z. Li, K. Zhu, Q. Zhao, A. Meng, The enhanced SERS effect of Ag/ZnO nanoparticles through surface hydrophobic modification, Appl. Surf. Sci. 377 (2016) 23–29.
[199] M.W. Brian, W.J. George, D. Nicolaas, C. Gerard, Surface-enhanced Raman spectroscopy competitive binding biosensor development utilizing surface modification of silver nanocubes and a citrulline aptamer, J. Biomed. Opt. 22 (7) (2017) 1–7.
[200] V. Montes-García, S. Rodal-Cedeira, M.J. Cordero-Ferradás, B. Gómez, L. García-Río, I. Pastoriza-Santos, J. Pérez-Juste, Pillar[5]arene-stabilized plasmonic nanoparticles as selective SERS sensors, Isr. J. Chem. 58 (11) (2018) 1251–1260.
[201] S. Wang, C.M. McGuirk, A. d'Aquino, J.A. Mason, C.A. Mirkin, Metal–organic framework nanoparticles, Adv. Mater. 30 (37) (2018) 1800202.
[202] H.R. Chandan, J.D. Schiffman, R.G. Balakrishna, Quantum dots as fluorescent probes: synthesis, surface chemistry, energy transfer mechanisms, and applications, Sensor. Actuator. B Chem. 258 (2018) 1191–1214.
[203] S. Shrestha, B. Wang, P. Dutta, Nanoparticle processing: understanding and controlling aggregation, Adv. Colloid Interface Sci. 279 (2020) 102162.
[204] J.B. Schlenoff, M. Li, H. Ly, Stability and self-exchange in alkanethiol monolayers, J. Am. Chem. Soc. 117 (50) (1995) 12528–12536.
[205] C. Chan, A.E. Carpenter, M. Gembicky, C.E. Moore, A.L. Rheingold, J.S. Figueroa, Associative ligand exchange and substrate activation reactions by a zero-valent cobalt tetraisocyanide complex, Organometallics 38 (7) (2019) 1436–1444.
[206] B. Fritzinger, I. Moreels, P. Lommens, R. Koole, Z. Hens, J.C. Martins, In situ observation of rapid ligand exchange in colloidal nanocrystal suspensions using transfer NOE nuclear magnetic resonance spectroscopy, J. Am. Chem. Soc. 131 (8) (2009) 3024–3032.
[207] G.H. Woehrle, L.O. Brown, J.E. Hutchison, Thiol-functionalized, 1.5-nm gold nanoparticles through ligand exchange Reactions: scope and mechanism of ligand exchange, J. Am. Chem. Soc. 127 (7) (2005) 2172–2183.
[208] E. Villarreal, G.G. Li, Q. Zhang, X. Fu, H. Wang, Nanoscale surface curvature effects on ligand–nanoparticle interactions: a plasmon-enhanced spectroscopic study of thiolated ligand adsorption, desorption, and exchange on gold nanoparticles, Nano Lett. 17 (7) (2017) 4443–4452.
[209] Y. Feng, S. Xing, J. Xu, H. Wang, J.W. Lim, H. Chen, Probing the kinetics of ligand exchange on colloidal gold nanoparticles by surface-enhanced Raman scattering, Dalton Trans. 39 (2) (2010) 349–351.
[210] C. Lee, R. Carney, K. Lam, J.W. Chan, SERS analysis of selectively captured exosomes using an integrin-specific peptide ligand, J. Raman Spectrosc. 48 (12) (2017) 1771–1776.
[211] X. Meng, J. Dyer, Y. Huo, C. Jiang, Greater SERS activity of ligand-stabilized gold nanostars with sharp branches, Langmuir 36 (13) (2020) 3558–3564.
[212] V. Dugandžić, S. Kupfer, M. Jahn, T. Henkel, K. Weber, D. Cialla-May, J. Popp, A SERS-based molecular sensor for selective detection and quantification of copper(II) ions, Sensor. Actuator. B Chem. 279 (2019) 230–237.
[213] A. Tycova, K. Klepárník, F. Foret, Bi-ligand modification of nanoparticles: an effective tool for surface-enhanced Raman spectrometry in salinated environments, Nanomaterials 9 (9) (2019).
[214] I. Bruzas, W. Lum, Z. Gorunmez, L. Sagle, Advances in surface-enhanced Raman spectroscopy (SERS) substrates for lipid and protein characterization: sensing and beyond, Analyst 143 (17) (2018) 3990–4008.
[215] Z. Zeng, Y. Liu, J. Wei, Recent advances in surface-enhanced Raman spectroscopy (SERS): finite-difference time-domain (FDTD) method for SERS and sensing applications, Trac. Trends Anal. Chem. 75 (2016) 162–173.
[216] H. Li, S. Liu, M.M. Hassan, S. Ali, Q. Ouyang, Q. Chen, X. Wu, Z. Xu, Rapid quantitative analysis of Hg2+ residue in dairy products using SERS coupled with ACO-BP-AdaBoost algorithm, Spectrochim. Acta Mol. Biomol. Spectrosc. 223 (2019) 117281.
[217] W. Ahmad, M.M. Hassan, J. Wang, M. Zareef, V. Annavaram, Q. Chen, An octahedral Cu2O@AgNCs substrate in liquid-microextraction coupled chemometric algorithms for SERS sensing of chromium(iii & vi) species, Analytical Methods 11 (47) (2019) 6004–6012.
[218] J. Zhu, A.A. Agyekum, F.Y.H. Kutsanedzie, H. Li, Q. Chen, Q. Ouyang, H. Jiang, Qualitative and quantitative analysis of chlorpyrifos residues in tea by surface-enhanced Raman spectroscopy (SERS) combined with chemometric models, Lebensm. Wiss. Technol. 97 (2018) 760–769.
[219] G. Chen, X. Lin, D. Lin, X. Ge, S. Feng, J. Pan, J. Lin, Z. Huang, X. Huang, R. Chen, Identification of different tumor states in nasopharyngeal cancer using surface-enhanced Raman spectroscopy combined with Lasso-PLS-DA algorithm, RSC Adv. 6 (10) (2016) 7760–7764.
[220] B. Buse, T. Berkay, B. Kemal, S. İhsan, O. Mehmet Cengiz, Genetic Algorithm-Driven Design of SERS-Active Surfaces for Early Detection of Diseases, Proc.SPIE, 2020.
[221] R. Hunter, A.N. Sohi, Z. Khatoon, V.R. Berthiaume, E.I. Alarcon, M. Godin, H. Anis, Optofluidic label-free SERS platform for rapid bacteria detection in serum, Sensor. Actuator. B Chem. 300 (2019) 126907.
[222] N. Banaei, J. Moshfegh, A. Mohseni-Kabir, J.M. Houghton, Y. Sun, B. Kim, Machine learning algorithms enhance the specificity of cancer biomarker detection using SERS-based immunoassays in microfluidic chips, RSC Adv. 9 (4) (2019) 1859–1868.
[223] S. Patze, U. Huebner, F. Liebold, K. Weber, D. Cialla-May, J. Popp, SERS as an analytical tool in environmental science: the detection of sulfamethoxazole in the nanomolar range by applying a microfluidic cartridge setup, Anal. Chim. Acta 949 (2017) 1–7.
[224] E.J.S. Brás, A.M. Fortes, T. Esteves, V. Chu, P. Fernandes, J.P. Conde, Microfluidic device for multiplexed detection of fungal infection biomarkers in grape cultivars, Analyst 145 (24) (2020) 7973–7984.
[225] W.Y. Lim, C.-H. Goh, T.M. Thevarajah, B.T. Goh, S.M. Khor, Using SERS-based microfluidic paper-based device (μPAD) for calibration-free quantitative measurement of AMI cardiac biomarkers, Biosens. Bioelectron. 147 (2020) 111792.